



This is to certify that the

thesis entitled

VIBRATION CONTROL IN "SMART" CANTILEVERED

BEAMS FEATURING FIBER-OPTIC SENSORS

presented by

Blane Patrick Hansknecht

has been accepted towards fulfillment of the requirements for

Masters degree in Mechanical Engineering

Major professor

Date 1 / 28 / 1991

LIBRARY Michigan State University

PLACE IN RETURN BOX to remove this checkout from your record. TO AVOID FINES return on or before date due.

DATE DUE	DATE DUE	DATE DUE
	·	

MSU Is An Affirmative Action/Equal Opportunity Institution c:\circ\detectus.pm3-p.1

# VIBRATION CONTROL IN 'SMART' CANTILEVERED BEAMS FEATURING FIBER-OPTIC SENSORS

Ву

Blane Patrick Hansknecht

## A THESIS

Submitted to
Michigan State University
in partial fulfillment of the requirements
for the degree of

**MASTER OF SCIENCE** 

Department of Mechanical Engineering

1991

#### ABSTRACT

# VIBRATION CONTROL IN 'SMART' CANTILEVERED BEAMS FEATURING FIBER-OPTIC SENSORS

# By Blane Patrick Hansknecht

This thesis work focuses on the development of 'smart' materials, which have the capability to sense their environment and to respond so as to optimize performance, using sensors and actuators incorporated into the structure of the material itself.

A review of the field of fiber-optic sensors is presented. Both polarimetric and interferometric fiber-optic sensors were investigated, and then imbedded within carbon-epoxy composite laminates, using improved preservation methods to protect the fiber sensors during the cure process. Standard, acrylate-coated optical fibers were shown to be sufficiently durable for such use. Frequency dependent phase shifts in polarimetric fiber-optic signals are characterized.

Research efforts involving actuators suitable for use in smart structures are also reviewed. Both polymeric piezoelectric distributed actuators and electrorheological (ER) fluids were used to control vibrations in cantilevered beams based on fiber-optic sensor signals. The reduction in the ER fluid effect with increasing shear strain is described. The amplitudes of forced vibrations were reduced by 80% at resonance with piezoelectric films, and by as much as 95% over a span of frequencies using ER fluids.

# **ACKNOWLEDGMENTS**

The author gratefully acknowledges the support and contributions of Dr. M.V. Gandhi and Dr. B.S. Thompson, as well as Corning Glassworks Inc. and Hercules Inc. for their donations of research materials.

#### **TABLE OF CONTENTS**

- I. LIST OF FIGURES, p. vi
- II. NOMENCLATURE, p. viii
- III. INTRODUCTION
  - A. 'Smart' Materials, p. 1
  - B. Motivation for Work and Applications, p. 6
    - 1. Why Smart Structures
    - 2. Why Fiber-optic Sensors
- IV. BODY OF THESIS
  - A. Background, p. 7
    - 1. Fiber-optic Sensors
      - a. Strain
      - b. Damage and Fatigue
      - c. Pressure
      - d. Temperature
      - e. Applications
    - 2. Actuators
      - a. Piezo-electric Ceramics and Polymers
      - b. Electro-rheological Fluids
      - c. Shape Memory Metals
      - d. Magnetostrictive Materials
      - e. Applications
  - B. Principles of Light Waveguides, p. 11
    - 1. Snell's Law
    - 2. Bend Losses
    - 3. Birefringence
    - 4. Polarization State
  - C. Interferometric Sensors and Light Interference Principles, p.15
    - 1. Mach-Zehnder
    - 2. Michelson
  - D. Polarimetric Sensors and Principles of Operation, p. 21
    - 1. Two-lead
    - 2. Single-ended

- E. Procedure for Imbedding Fiber-Optic Sensors in a Polymeric Composite Laminate, p. 25
  - 1. Composite Manufacture Process
    - a. Lay-up
    - b. Curing
  - 2. Imbedding Fiber-optic Sensors
    - a. Orientation
    - b. Protection
  - 3. Effect of Curing on Performance
- F. Actuators, p. 30
  - 1. Piezo-Electric Films and Ceramics
    - a. Principles of Operation and Applications
    - b. Advantages vrs Drawbacks
  - 2. Electro-Rheological (ER) Fluids
    - a. Principles of Operation and Applications
    - b. Advantages vrs Drawbacks
  - 3. Shape Memory Metals, Magneto-Strictive Materials, and Other Potential Actuators
    - a. Principles of Operation and Applications
    - b. Advantages vrs Drawbacks
- G. Control Algorithms, p. 36
  - 1. Phase-based for Piezo-Electric Actuators
  - 2. Frequency-based for ER Fluid Actuators
  - 3. Robust, Amplitude-based for ER Fluid Actuators
- H. Experimental Program, p.39
  - 1. Goals
  - 2. Experimental Procedures
  - 3. Results and Accomplishments
- V. CONCLUSIONS, p. 49
- VI. RECOMMENDATIONS, p. 51
- VII. REFERENCES p. 53

#### LIST OF FIGURES

- Figure 1: Light Propagation in Single- and Multi-Mode Optical Fibers.
- Figure 2: Interference Fringe Patterns Falling On Slitted Photodiodes.
- Figures 3-7: Frequency Dependent Phase Shift in Fiber-Optic Signal:

  A Comparison With the Signal of a Displacement Sensor
  Located at the Beam Tip, For 16, 18.5, 25, 55, and 88.5 Hz.
- Figure 8: Composite Lay-Up for Curing Process.
- Figure 9: Imbedding Fiber-Optic Sensors in Polymeric Composite Laminates.
- Figure 10: Fiber-Optic Sensor Imbedded in Carbon-Epoxy Composite Plate.
- Figure 11: Imbedded Single-Ended Polarimetric Fiber-Optic Sensor Signal.
- Figure 12: Photomicrograph of ER Fluid at 0.0 kV/mm and at 2.0 kV/mm.
- Figure 13: ER Fluid Sandwich Beam Structure.
- Figure 14: Frequency Response Curves of an ER Beam with 0.0 kV/mm vrs 2.0 kV/mm Applied Voltage.
- Figure 15: ER Beam Frequency Shift and Damping Increase with Increasing Applied Voltage.
- Figures 16-18: Reduction in ER Fluid Effect with Increasing Magnitudes of Vibration for 3.0 kV/mm, 2.0 kV/mm, and 1.0 kv/mm Applied Voltages.
- Figure 19: Robust Closed-Loop Control in an ER Fluid Beam by Amplitude Scanning Over Several Voltage Levels.
- Figure 20: Fiber-Optic Sensor Configurations.

- Figure 21: Mach-Zehnder Interferometric Fiber-Optic Sensor Optical Set-Up.
- Figure 22: Polarimetric Fiber-Optic Sensor Optical Set-Up.
- Figure 23: Idealized Interferometric Fiber-Optic Signal with Cantilever Beam Tip Deflection.
- Figure 24: Surface- Bonded and Imbedded Fiber-Optic Sensor Equipped Carbon-Epoxy Composite Beams.
- Figure 25: Smart Structure Experimental Set-up.
- Figure 26: Photograph of Smart Structure Experimental Apparatus.
- Figure 27: Comparison of Single-Ended Polarimetric Fiber-Optic Sensor Signal with Non-Contacting Displacement Sensor at Beam Tip for Small Excitation Amplitudes at Resonance (41.2 Hz).
- Figure 28: Same as Figure 27, but Low-Pass on a Bandpass Filter Set to 110 Hz to Filter Noise from 120 Hz Overhead Lights.
- Figure 29: Comparison of Frequency Response Curves Generated Using Proximeter and Polarimetric Fiber-Optic Sensor Signals.
- Figure 30: Phase-Based Control Algorithm Response to Tip Velocity Signal.
- Figure 31: Forced Response as Phase-Based Closed-Loop Control Begins.
- Figure 32: Normalized Vibration Amplitude vrs Excitation Frequency for Comparison of Natural Response vrs Smart Structure Response.

# **NOMENCLATURE**

#### INTRODUCTION

One traditional measure of the progress of humanity has been by the materials they have used, thus the progression: stone age, iron age, bronze age. 'Smart' materials represent a new generation following the synthetic materials age. They are characterized by their ability to sense their environment and to react so as to perform optimally for a given set of conditions. Class I smart materials are passive, featuring a microsensor system, Class II smart materials are active, with imbedded actuators in addition to imbedded sensors, and Class III smart materials are intelligent, adding adaptive learning capabilities. Unless stated to the contrary, any further references to 'smart' materials or structures should be understood to refer to Class II smart materials. This thesis brings together research in fiber-optic sensors, their incorporation into polymeric composite laminates, various actuators, and closed-loop control programs to produce Class II smart materials.

The following section of this thesis reviews the fields of fiber-optic sensors and of suitable actuators for use in smart materials. The next sections explain the propagation of guided light and light interference principles, thus, how interferometric fiber-optic sensors function. A model for polarimetric fiber-optic is also presented. A procedure for imbedding fiber-optic sensors in polymeric composite laminates is described. The characteristics, advantages, and drawbacks of piezo-electric films, electrorheological fluids, and other potential actuators are addressed. Finally, an experimental program uses these sensors and actuators, with control algorithms, to reduce the amplitude of vibration in cantilevered

beams. The remainder of this introduction is devoted to a discussion of the attributes and types of fiber-optic sensors.

The development of fiber-optic sensors has taken place almost entirely in the last fifteen years, and their use in the area of smart materials is more recent yet. Even so, fiber-optic sensors are already successfully competing with conventional sensors. Fiber-optic sensors exhibit a number of advantages over other sensors. They are extremely lightweight, therefore, less intrusive than accelerometers, for example. Since the waveguide is dielectric, they are immune to electromagnetic interference, and yet could still be used to detect magnetic fields by coating the fiber with a magnetostrictive material. They can also be used to detect temperature, pressure, strain and vibration. Vibration control in large space structures is one case where fiber-optic sensors are achieving success.

Perhaps the greatest advantage that fiber-optic sensors have for smart structures applications is their ability to be imbedded directly in fibrous polymeric composite materials. This enables the monitoring of conditions within the structure. The cure process can be optimized, and the fibers can remain as life-long sensors protected by the structure around them.

Structural sensors are already used in high stress applications such as military aircraft to warn pilots when the integrity of the plane is endangered or compromised. The sensors used are typically strain gauges, which are subject to debonding and can only detect strain or damage over a small

region. Fiber sensors, on the other hand, could be incorporated into the structure of the plane and sense strain or damage over considerable lengths.

On commercial flights, this early damage detection would be an invaluable safety feature for preventing crashes caused by fatigue failure, which inspection crews can overlook, as occurred on the tragic Aloha flight in 1989.

The term 'fiber sensor' used so far actually covers a number of optical fiber-based sensor configurations including attenuation-based sensors, polarimetric-based sensors, interferometric-based sensors, and sensors relying on specialty fiber coatings; furthermore, each of the above sensor categories consists of a number of subcategories. Other fiber sensors rely on optical time-domain reflectometry, which detects backscattered light from defects and environmental effects such as bending. The Pockels effect may be used to introduce birefringence for measuring voltages.

Attenuation-based sensors typically rely on a physical mechanism of some sort which induces microbending in the optical fiber when the structure that the fiber is to monitor is disturbed. The microbends cut off an amount of the light passing through the fiber in a manner analogous to pinching a garden hose to stop the water from flowing. This method has the advantage that since the only feature of interest in the light guided by the fiber is its intensity, no laser is required. Less costly photodiodes, and inexpensive, easy to handle multimode fibers may be used. The disadvantages of this method are lower sensitivity than other methods, and the need for some means of

inducing the microbending, which is at odds with the smart materials philosophy of incorporating the sensor within the structure it is to monitor.

A better smart materials approach using an attenuation-based sensor has been proposed<sup>1</sup>, which imbeds a fiber in a composite material in order to signal when the material has suffered serious fatigue or impact damage. The fiber has its protective coating etched off at regular intervals so that its failure strength approximates the failure strength of the material of which it is a part. If the material is damaged, the fiber breaks, resulting in a noticeable drop in the intensity of the light passing through the fiber. This application has the advantages of the previous method without the disadvantages. It is limited, though, by the fact that it is a one-time sensor designed only to warn of impending failure. It cannot be used to monitor the structure or its environment during normal use.

Polarimetric and interferometric fiber-optic sensors can be used to measure the vibration, strain, and/or heat of the structure they are bonded to or imbedded in, to allow self-actuated control of an intelligent structure in response to the environment it senses. Because these sensors operate by detecting changes in the phase or polarization state of light, not just the intensity, they require a laser source and single-mode optical fiber. These sensors are readily adaptable for imbedding in a composite structure and are also more sensitive than attenuation-based sensors. Both of these sensors will be discussed in greater detail in the body of this thesis.

There are, in addition, interferometric sensor configurations which were not considered in the research of this thesis: Fabry-Perot, Sagnac, Bragg, and modal interferometers. Fiber-optic Fabry-Perot sensors require sensitive splicing techniques and are more fragile than other sensors. Modal interferometers are less sensitive than other interferometers and require specialized fiber. An excellent review of various fiber-optic sensors is given by Turner, et al<sup>2</sup>.

Experimental and postulated specialty coating fiber sensors operate on the same general principal as one of the above sensors, except that the modification of the light passing through the fiber is caused by coatings on the fiber. For example, by coating a fiber with a magneto-strictive material, the strength of magnetic fields can be detected: the field induces a contraction or expansion of the magneto-strictive material, which strains the fiber, resulting in a detectable modification of the light passing through the fiber. Similarly, electric voltages could be detected by a fiber coated with a piezo-electric polymer. Even various chemicals could be detected by coating the fibers in a phosphorescing substance, and observing the intensity of light produced by the coating (in the presence of certain chemicals) and transmitted through the fiber. Since the fiber itself is glass, the sensor is chemically inert.

Other coatings, especially polyimides, are under study for protecting fibers that are to be imbedded in composites. During the cure cycle, polyimide coated fibers are subject to less loss of mass, and the lifetime of the polyimide-coated fiber is greater than that of untreated fibers, according to R.O. Claus, et al<sup>3</sup>.

## Motivation for Work and Applications

# Why use smart structures?

- reacts to environmental stimuli without the need for human intervention to achieve optimal state: minimize vibrations, alter dimensions, change work path, etc.

Why use fiber-optic sensors in smart structures?

- lightweight
- very small
- inert, corrosion resistant
- can integrate measurements over a large area
- sensitive
- immune to electromagnetic interference
- multifunctional: databus compatible
- signal processing by integrated optics
- can be multiplexed
- no electrical or fire hazard
- suitable for imbedding in composites
- Applications:
  - sense strain, vibration, temperature, and pressure
  - measure magnetic and electric fields
  - cure monitoring
  - impact sensing
  - thermal mapping
  - monitor structural integrity
  - damage detection
  - fatigue life evaluation

#### A. BACKGROUND

The primary goal of this investigation is to imbed fiber-optic sensors into a composite structure which incorporates actuators such as electro-rheological fluids or piezo-electric polymeric films in order to form a "smart structure," a structure that reacts to the environment it senses in an autonomous manner. Previous studies have developed the use of optical fiber in sensors, and have imbedded the fibers in composites, but no work to date has used the above in conjunction with suitable actuators and control algorithms to produce an integrated self-actuating "smart structure". The actuators that were used in this thesis work were piezo-electric polymeric thin films and electro-rheological fluids. Other actuators suitable for "smart structures" include piezo-electric ceramics, shape memory metals, and magnetostrictive materials.

#### A.1 Fiber-Optic Sensors Background:

The field of fiber-optic sensors is extensive. R.M. Measures, R.D. Turner, W. D. Hogg, et al, have published fiber-optic sensor papers on strain detection<sup>4</sup>, damage detection<sup>1</sup>, imbedded sensors<sup>5</sup>, and the merits and drawbacks of the various classes of fiber-optic sensors<sup>2</sup>. The earliest paper that investigated imbedded fiber-optic sensors in polymeric composite materials was done by S.Y. Field and K.H.G. Ashbee in 1972<sup>6</sup>. Other authors involved in researching strain detection include S.R. Waite, et al<sup>7</sup>, R. Rogowski,

et al<sup>8</sup>, and M. Martinelli<sup>9</sup>. Waite, et al, are also active in detecting damage and fatigue in composites with fiber-optic sensors<sup>10</sup>. Pressure and temperature sensing using fiber-optic sensors has been researched by G.B. Hocker<sup>11</sup>, and by N. Lagakos and J.A. Buccaro<sup>12</sup>, and R.W. Griffiths<sup>13</sup>. Bragg fiber-optic sensors have been developed by G. Meltz, W.W. Morey and W.H. Glenn<sup>14</sup>.

The use of fiber-optic sensing of vibrations is treated in a paper by Spillman<sup>15</sup>.

In the area of fiber coatings there are papers on a spectrum of potential applications, from how coatings affect microbending losses, by E.H. Urruti and J.F. Wahl<sup>16</sup>, to luminescent coated fibers for chemical sensing, by K. Liu, et al<sup>17</sup>. Claus, et al, are also investigating coatings for imbedded fiber-optic sensors, for the purpose of protecting the sensor during cure and extending the lifetime of the fiber<sup>3</sup>.

In this thesis work, several varieties of fiber-optic sensors were investigated, including a Mach-Zehnder interferometric sensor, a Michelson interferometric sensor, a polarimetric sensor, and a single-ended variation of the polarimetric sensor. Each of these will be discussed in detail in the body of the thesis, with regard to both technical explanation and suitability for meeting the chief purpose of this thesis work.

# Piezo-Electric Actuators Background:

Several papers by E.F. Crawley, et al, investigate the use of piezoceramics as actuators 18-20. Crawley used piezoceramics to induce strain in beams to control structural deformations to verify the analytical models that he developed. Pennwalt Company's Kynar Piezo FilmTechnical Manual is a valuable information source on the characteristics of polymeric piezo-electric films<sup>21</sup>.

Vibration control is addressed in papers by J.E. Hubbard Jr. and T. Bailey <sup>22</sup>, by Ikegami, et al<sup>23</sup>, and by A. Baz and S. Poh<sup>24</sup>. These papers considered optimal actuator positions, distributed-parameter actuator and control models, and bonding layer effects for minimizing vibration amplitudes in cantilevered beams with piezo-electric actuators.

### Electro-Rheological Fluids Background:

The primary published work in electro-rheological fluids is in the papers by M.V. Gandhi and B.S. Thompson<sup>25-26</sup>. A mathematical model for a cantilevered beam with a viscoelastic layer (as used in the experiments by Gandhi and Thompson) can be found in a paper by C.T. Sun, et al<sup>27</sup>. So far, however, no model exists which also includes the electro-rheological fluid characteristics.

## Other Suitable Actuators:

Magnetostrictive materials are being manufactured by companies such as

Edge Technologies and work in a manner analogous to piezoelectric materials,

except the strain is induced by a magnetic field instead of by a voltage field.

Like piezoceramics, magnetostrictive materials are brittle, however, there are

less safety concerns since high voltages are not needed.

Shape-Memory alloys are metals that return to a preset, trained shape from whatever deformed state they are in, as described by material data from Memory Metals Incorporated, for example. Use of shape-memory metals as both actuators and sensors has been conducted by authors such as C.A. Rogers<sup>28</sup> and R. Ikegami, et al<sup>23</sup>.

## B. Principles of Light Waveguides

Optical fibers consist of a very thin core of glass, surrounded by a cladding of a glass with a slightly lower index of refraction. This fiber is typically protected further by an acrylate or a polyimide coating, and often one or more of these fibers are contained within a multi-layered jacket. The only essential parts for guiding light, however, are the core and the cladding.

The light is guided along the core by internal reflection according to the well-known Snell's Law:

$$n_1 * \cos(\theta_1) = n_2 * \cos(\theta_2)$$
 (1)

where  $n_1$  and  $n_2$  are the indices of refraction of the core and cladding, and  $\theta_1$  and  $\theta_2$  are the angles of incidence and reflection, respectively.

The light entering the fiber must be within certain angles to pass along the core. This is termed the Numerical aperture (NA) and varies depending upon the geometry and material characteristics of the fiber. A multi-mode fiber has a core large enough (typically 50-100  $\mu$ m) to allows light to pass along it in any of several paths. A single-mode fiber has a core small enough (approximately 8  $\mu$ m) that light can only travel along one path. This is shown graphically in figure 1.

One can see from Snell's Law that where there are bends in the fiber the light guided along the core is more likely to pass into the cladding due to the change in the angle at which the light interacts with the core-cladding

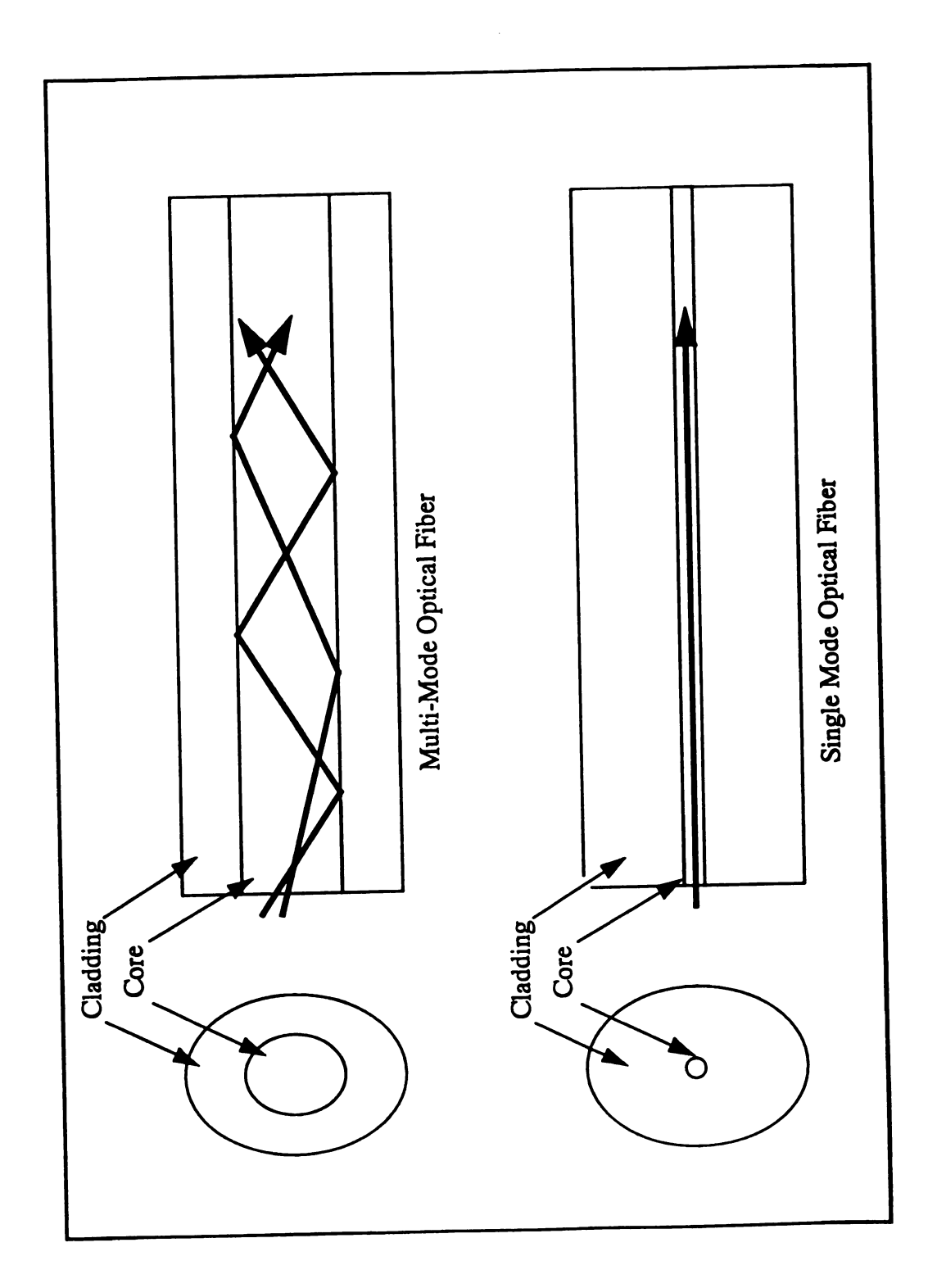


Figure 1: Light Propagation in Single- and Multi-Mode Optical Fibers

interface. In multimode fibers, bends are sometimes introduced to exploit this in order to strip higher order modes from the core. In single mode fibers this loss is wavelength dependent, and may be expressed by

$$\gamma = 10 \operatorname{Log} \left[ R\Delta(\alpha + 2) / (2\alpha * a) \right], \qquad (2)$$

where R is the bend radius (several centimeters or less),  $\alpha$  is a profile parameter,  $\Delta$  is the index elevation, and a is the core radius.

There are two possible orthogonal polarization states for light passing through a single-mode fiber. Polarized light may be coupled to the single mode fiber in a way that excites both polarization states equally. A single mode fiber with a perfectly circular cross-section will have light propagate equally in both of these orthogonal modes. If, however, the fiber were ellipsoid in cross-section instead, the light along one mode would propagate at a different speed than the light in the other mode, on account of the difference in path lengths between them. The difference between the effective refractive indices of these two modes is the birefringence of the fiber. In addition, the birefringence can be introduced due to perturbations to the fiber, because strain will alter the fiber cross-sectional geometry. The amount of birefringence introduced is dependant on the manner in which strain is coupled to the fiber.

For a fiber between two plates, a linear force, f, will introduce a birefringence

$$\beta_f = 4 C_s f / (\pi r E),$$
 (3)

where r is the fiber outer radius, E its Young's modulus, and

Cs = 
$$0.5 k_0 n_0^3 (p_{11} - p_{12}) (1 - v_0)$$
.

Here,  $n_0$  is the average fiber refractive index,  $\upsilon_p$  is Poisson's ratio,  $p_{11}$  and  $p_{12}$  are strain-optical tensor components of the fiber, and  $k_0 = 2\pi / \lambda_0$ , and  $\lambda_0$  is the free space wavelength.

When forces are distributed over the surface of the fiber instead of point loading, however, as is the case for fibers imbedded in fibrous composites, equation (3) may be errant by up to a factor of  $8/\pi$ .

For an optical fiber that runs parallel to the fiber direction of the two composite prepreg plys it is sandwiched between, a more appropriate model may be that of a fiber pressed into a V-groove of angle  $2\delta$ 

$$\beta_V = 2 C_s f (1 - \cos 2\delta \sin 2\delta) / (\pi r E)$$
. (4)

Equasions (3) through (4) can be found in a paper by S.C. Rashliegh<sup>29</sup>. An optical fiber running orthogonally to the fiber direction of the prepreg plys will experience a series of small kinks, and so will have still a different birefringence. From this, it is obvious that the birefringence introduced into a fiber-optic sensor imbedded in a composite structure will vary with the orientation of the sensor with respect to the adjacent ply fiber directions.

An ideal fiber without flaws such as elliptical or varying cross-section, material point defects, varying index of refraction, or bends and twists in the fiber will maintain the initial polarization state introduced to the fiber. Real

fibers have imperfections that result in coupling between the two orthogonal modes. Coupling from one polarized mode to the other completely will occur if a perturbation matches the criterion

$$|\beta_x - \beta_y| = k + \Delta k$$

where k is the spatial frequency of the perturbation along the length of the fiber,  $\Delta k$  is the spatial frequency of the length of the fiber, and  $\beta_x$ ,  $\beta_y$  are the propagation constants of the two orthogonal modes. Thus, changes in any perturbations to the fiber will result in changes in the polarization state of the light guided by the fiber. Energy is coupled from one mode to another and hence, the intensity of light passing along a particular mode will change.

### C. Interferometric Sensors and Interference of Light Principles

The interference of light is a well established property. When two coherent beams of light interact there results alternating regions of constructive and destructive interference, leading to fringes of light and dark bands, respectively. Beams are coherent if they propagate in step, although they may be out of phase. This interference is described by the superposition principle. Any changes in the phase of one beam relative to the other result in a shift in the interference fringes. A 180 degree change in the relative difference in phase, for example, will result in a fringe shift such that the positions previously occupied by the dark fringes are now held by light fringes, and vice versa. Since the wavelength of coherent sources is extremely short, (633 nm for a Helium-Neon Laser, for example) the end result is that extremely small changes in the relative phase can be observed by the shift in the macroscopic interference fringes. The interference of two waves is treated in greater detail below.

The interference of light assumes that light has wave-like nature. A solution to the differential wave equation has the form

$$E(x,t) = E_0 \sin[\omega t - (kx + \varepsilon)]$$
 (5)

where  $E_0$  is the amplitude of the light,  $\omega$  is its angular frequency, k is a propagation constant, and  $\varepsilon$  is an initial phase angle. When two such waves occupy the same space, the resulting disturbance is a linear superposition of

the two

$$E = E_{01} \sin[\omega t - (kx_1 + \varepsilon_1)] + E_{02} \sin[\omega t - (kx_2 + \varepsilon_2)]$$
 (6)

expanding:

$$E = E_{01} \left( \sin[\omega t] \cos[kx_1 + \varepsilon_1] + \cos[\omega t] \sin[kx_1 + \varepsilon_1] \right)$$

$$+ E_{02} \left( \sin[\omega t] \cos[kx_2 + \varepsilon_2] + \cos[\omega t] \sin[kx_2 + \varepsilon_2] \right)$$
 (7)

rearranging:

$$E = (E_{01} \cos[kx_1 + \varepsilon_1] + E_{02} \cos[kx_2 + \varepsilon_2]) \sin[\omega t] + (E_{01} \sin[kx_1 + \varepsilon_1] + E_{02} \sin[kx_2 + \varepsilon_2]) \cos[\omega t] .$$
 (8)

Next, substitute  $E_0 \cos[kx + \varepsilon]$  for the terms in the first set of parentheses in the above equation, and  $E_0 \sin[kx + \varepsilon]$  for the terms in the second set.

$$E_0 \cos[kx + \varepsilon] = E_{01} \cos[kx_1 + \varepsilon_1] + E_{02} \cos[kx_2 + \varepsilon_2]$$
 (9)

$$E_0 \sin[kx + \varepsilon] = E_{01} \sin[kx_1 + \varepsilon_1] + E_{02} \sin[kx_2 + \varepsilon_2]$$
 (10)

This substitution is valid, provided the following expressions solving for  $E_0$  and  $[kx + \varepsilon]$  are met:

$$E_0 = [E_{01}^2 + E_{02}^2 + 2E_{01}E_{02}\cos[k(x_1-x_2) + (\varepsilon_1 - \varepsilon_2)]]^{1/2}$$
 (11)

and

$$[kx + \varepsilon] = tan^{-1} \frac{E_{01} \sin[kx_1 + \varepsilon_1] + E_{02} \sin[kx_2 + \varepsilon_2]}{E_{01} \cos[kx_1 + \varepsilon_1] + E_{02} \cos[kx_2 + \varepsilon_2]} . \tag{12}$$

Equation (11) is obtained by squaring and adding equations (9) and (10), and equation (12) is obtained by dividing equation (10) by equation (9). As long as equations (11) and (12) are met for  $E_0$  and  $[kx + \varepsilon]$ , the summation of the

two waves becomes

$$E = E_0 \cos[kx + \varepsilon] \sin[\omega t] + E_0 \sin[kx + \varepsilon] \cos[\omega t]$$
 (13)

or

$$E = E_0 \sin[\omega t + kx + \varepsilon] . \tag{14}$$

A phase difference between the two waves may be introduced in two ways: by the difference in the initial phase angles, or by a difference in the path length traversed by the two waves. Coherent waves have  $\varepsilon_1$  -  $\varepsilon_2$  constant, and equal if emitted in phase, as is the case for two beams from a single source. In this case, the phase difference  $\delta$  is

$$\delta = k(x_1 - x_2) = 2\pi \, n(x_1 - x_2) / \lambda_0 \tag{15}$$

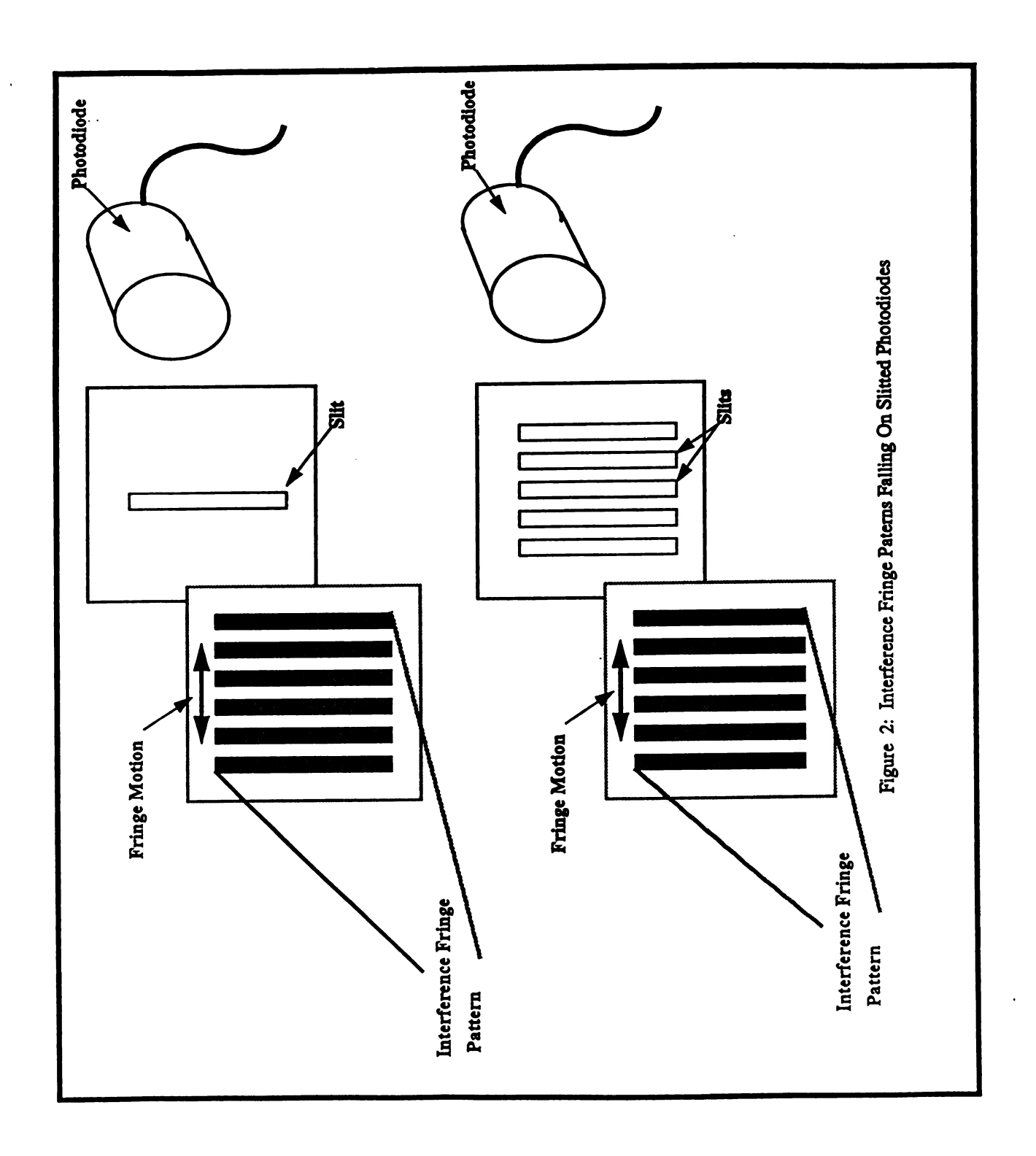
where  $\lambda_0$  is the free space wavelength and n is the index of refraction of the medium the waves are traveling through. From equation (11), it follows that when  $\delta$  equals an even multiple of  $\pi$  the amplitude of the combined waves will be at a maximum, and when  $\delta$  equals an odd multiple of  $\pi$  the amplitude of the combined waves will be at a minimum. This is referred to as constructive and destructive interference, respectively. Since the wavelength of the source may be very small (633 nm for a HeNe laser, for example), very minute changes between the path lengths can be detected by the resulting shift in the fringes.

#### C.1 The Fiber-optic Mach-Zehnder Interferometer

Interferometric sensors exploit the principle of the interference of light.

Two coherent beams are formed, often by beam splitting. In a fiber-optic Mach-Zehnder set-up, these beams are coupled into two single mode fibers, called the reference arm and the sensing arm. Any strain on the fiber waveguide results in a change in the length of the fiber and, hence, a change in the path length of the light guided by the fiber. When the sensing arm experiences strain not seen by the reference arm, there is a relative change in path length of the light passing along the sensing arm with respect to the reference arm. This results in a relative phase shift between the two guided beams, which may be detected by combining the beams and observing the shift in the fringe pattern. In a Mach-Zehnder this is accomplished by superimposing the beams as they exit the fibers with the aid of a beam splitting cube. The resulting fringe pattern falls on a slitted photodiode, so that unit-impulse-like signals may be obtained as each bright fringe shifts across the face of the slit. To improve the strength of this signal, a multiple slit filter was manufactured to cover the face of the photodiode, and this detector was positioned such that fringes of the same kind were aligned with each slit of the multiple slit array (see figure 2).

Since strain is defined as the change in length per unit length, it follows that the change in path length for light passing through the sensing arm with respect to the light guided by the reference arm will depend on the difference between the lengths of these two arms subject to the strain. Hence a fiber-optic interferometer can approximate point sensing when the difference between



the arms is small, or the sensor can integrate the strain over large lengths by increasing the difference in length between the arms, to the limit imposed by the coherence length of the light source.

#### C.2 The Michelson Fiber-optic Interferometric Sensor

The Michelson fiber-optic sensor differs from the Mach-Zehnder in that the light does not simply exit through the opposite end of the fiber from which it was coupled. Instead, that end is mirrored to reflect the light guided by the fiber so the light travels back along the length of the fiber and is decoupled by the same apparatus that initially coupled it to the fiber. This variation is more elegant than the Mach-Zehnder since it reuses the coupling apparatus rather than requiring such devices at both ends of the sensing fiber and the reference fiber. Also, when imbedding the sensor in a composite structure, the Michelson sensor requires only two leads, one for each arm of the interferometer, whereas the Mach-Zehnder requires four, since the far end of the fibers must also be lead out of the composite to recover the signal. For a cantilevered beam it is desirable to have all the leads exit from the same end of the beam, so leads exiting from the free end of the beam are not shaken wildly with the tip deflections. For the Mach-Zehnder interferometer this requires the sensing and reference arms to double back, producing twice the inter-ply disturbance to the composite as the Michelson interferometer, as well as requiring a bend in the arms of the sensor where they double back. This bend causes a loss in signal strength since the increase in the angle of incidence of light guided by

there is a minimum bend radius for optical fibers, typically of several millimeters, therefor the Mach-Zehnder sensor has a minimum width requirement that the Michelson sensor does not have. Finally, since the light guided in the Michelson sensor travels the length of the fiber twice, the Michelson is twice as sensitive as the Mach-Zender for the same sensing length of fiber.

The only drawback to the Michelson sensor is the need to apply silver to one end of the fiber, and this silver can be subject to debonding from the glass fiber.

As long as both arms of an interferometric fiber-optic sensor are subject to the same disturbances (i.e. temperature changes, vibrations, etc.) in the region away from the sensing region, the effects of the disturbance will be negated, since light traveling in each arm will be modified identically. Thus, there are no changes in the fringe pattern due to these effects, and the sensor is said to be lead-insensitive. The sensing region is made sensitive by having the length of the two arms different in the region. For a Mach-Zehnder interferometer, a loop is typically made by each arm, with one loop being larger than the other. The Michelson interferometer, however, simply needs one arm to be longer than the other since it is single-ended.

#### D. Polarimetric Sensors and Principles of Operation

Polarimetric sensors do not operate on the interference principles that the interferometric sensors do. Instead, the polarization state of the light that propagates along the fiber is the property that is of interest. Single mode optical fiber allows two orthogonal polarization states to propagate simultaneously. In an ideal fiber the light carried by each mode throughout the length of the fiber is the same as the light originally coupled into each of the modes. However, when imperfections are introduced, due to strain on the fiber, or non-uniformities in the material of the waveguide, for example, light may be coupled from one mode to the other. The amount of light that changes modes depends on the magnitude of the strain and the length of the fiber subject to the strain.

In a polarimetric sensor, polarized light is coupled into a single mode fiber, usually so both modes of the fiber are equally excited. The light exiting the fiber is passed through a polarizer. A polarizer allows light to pass, but only light whose electric field parallels the orientation of the polarizer. In other words, only the component of polarized light that has the same orientation as the polarizer is passed. Thus, the polarizer can be positioned so that it allows the passage of all of the light from one of the two orthogonal modes of the fiber and none of the light from the other mode. This allows a photodiode with the polarizer to detect the change in energy in a mode as light couples in or out of the mode due to strain on the fiber.

A model for a polarimetric sensor is presented below, as described by Spillman and Kline<sup>15</sup>. Polarized light coupled into a fiber is expressed as

$$\mathbf{E}_{\rm in} = \mathbf{E}_0 \begin{bmatrix} \cos \theta \\ \sin \theta \end{bmatrix}, \tag{16}$$

where  $\theta$  is the angle of the polarization with respect to the stress on the optical fiber. The fiber is modeled as a transformation matrix,

$$[R] = \begin{bmatrix} e^{i(\beta/2)\cos\omega} & -e^{i(q/2)\sin\omega} \\ e^{-i(q/2)\sin\omega} & e^{-i(\beta/2)\cos\omega} \end{bmatrix}, \qquad (17)$$

where q is the retardation of the coupled light,  $\omega$  is the percentage of light coupled from on orthogonal polarization mode to the other, and  $\beta$  is the phase lag between the two. This phase difference is a function of the orthogonal radial components of applied stress,  $\sigma_x$  and  $\sigma_y$ , the length of the fiber subject to the stress, L, the wavelength of the light,  $\lambda$ , and the strain-optic constant, Cs, as shown in the following equation:

$$\beta = \beta_0 + 2 \pi L Cs (\sigma_x - \sigma_v) / \lambda.$$
 (18)

In the polarimetric sensor, light exiting the fiber passes through an analyzing polarizer, which is modeled by

$$[S] = \begin{bmatrix} \cos\psi & \sin\psi \\ -\varepsilon\sin\psi & \varepsilon\cos\psi \end{bmatrix}, \tag{19}$$

where  $\epsilon^2$  is the extinction ratio of the polarizer and  $\psi$  is the angle of its transmission axis. Hence, the output light which falls on the photodiode can be determined by

$$\mathbf{E}_{\text{out}} = [S] [R] \mathbf{E}_{\text{in}}. \tag{20}$$

For a polarimetric system where the input polarization angle and the output polarizer angle are set to 45 degrees, assuming that the output light is linearly polarized ( $\varepsilon = 0$ ) and there is no mode coupling ( $\omega = 0$ ) results in the following expression for the output power:

$$I_{out} = .5 E_0^2 (1 - \cos \beta)$$
 (21)

Thus, the intensity of the light on the photodiode is a function of  $\beta$ , which in turn varies with the applied stresses on the optical fiber guiding the light.

Polarimetric sensors are not as sensitive as interferometric sensors. Also, they are more difficult to localize. The leads can be made insensitive, however, by using high-birefringent fiber spliced to the fiber in the sensing region<sup>4</sup>.

The polarimetric sensors do hold advantages over interferometric sensors, however. They do not require a sensing arm, so the number of leads is halved. This reduces the handling required in assembling the fiber, lowers the chance of damaging the sensor during manufacture and use, and lowers the intrusiveness of the sensor when it is imbedded in polymeric composite structures. Like the Michelson fiber-optic interferometric sensor, the end of a polarimetric sensor can be mirrored, allowing for a single-ended configuration. This type of polarimetric sensor only requires one lead. The sensitivity, although lower than the highly sensitive interferometers, is sufficient for the purposes of vibration control considered herein.

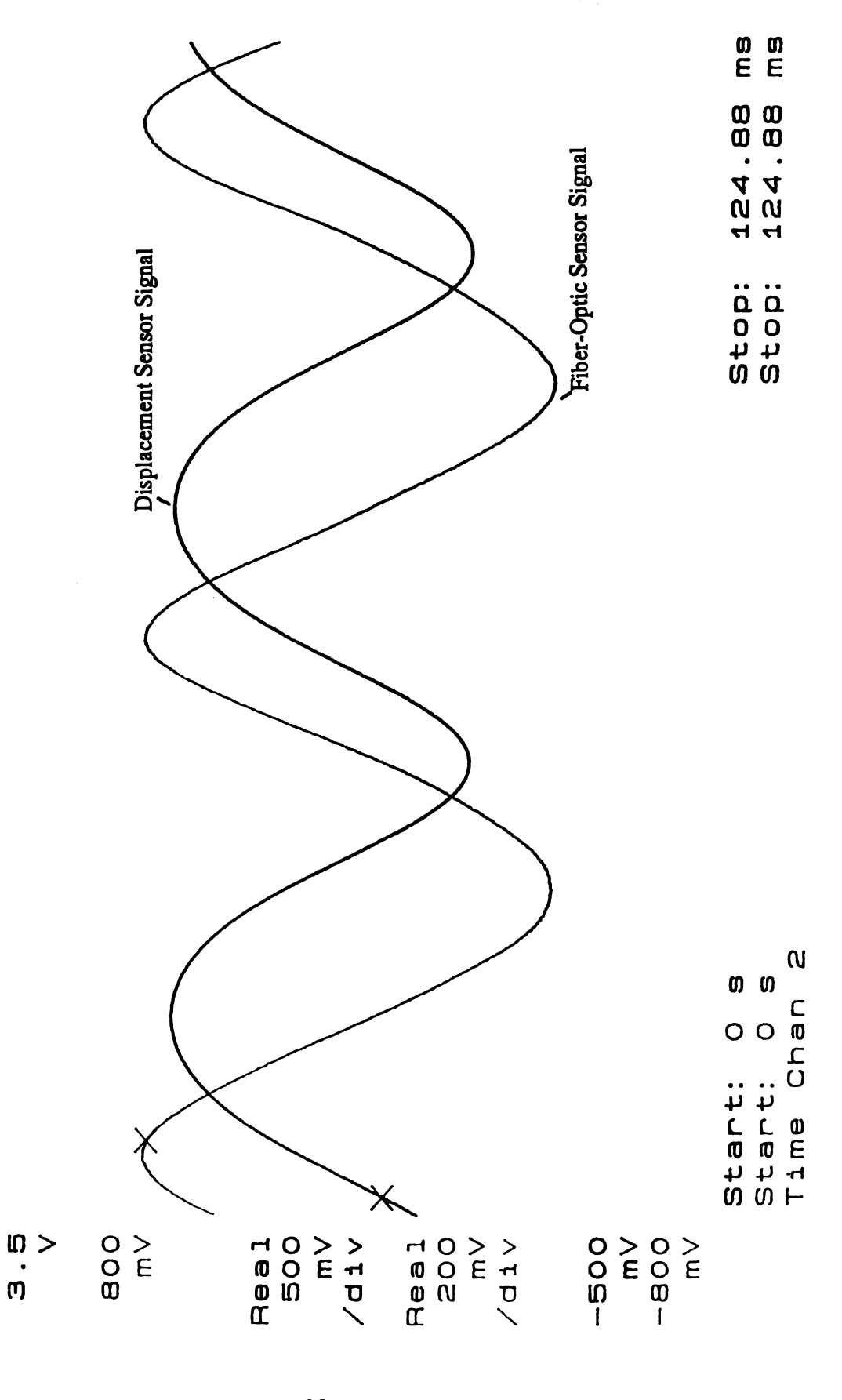
Finally, and most important from a controls point of view, the signal is readily usable. The signal varies with strain integrated over the sensing

length. Thus, it varies with the displacement of the cantilevered beam, differing only in phase. For large lengths of fiber subject to strain, however, it is possible that some of the light coupled out of one polarization state could be coupled back in; this could result in erroneous frequency values from the sensor, although this effect was not observed in any of the experiments of this thesis. In contrast to the polarimetric signal, the signal from an interferometric sensor is a series of pulses whose frequency is proportional to the rate of strain. This requires a program to count the impulses and the spacing between them, determine from the spacing the cycle length, and calculate the frequency. This is a difficult task to do accurately, and very difficult to accomplish in the limited time available for real-time control of vibration.

The polarimetric sensor is a distributed strain sensor - it integrates the strain over its sensing length. This results in a frequency dependant phase shift in the polarimetric signal. The polarimetric fiber-optic sensor accurately measures the frequency of excitation of the structure it monitors, but the phase of this signal varies between the phase of the acceleration and the phase of the velocity, as shown in figures 3-7. This is similar to the phase shift seen in a displacement sensor signal of an oscillating cantilevered beam when the sensor is moved from the tip of the beam towards the base of the beam. The phase shift in the polarimetric sensor varies depending on the sensor length.

**တ** တ ဧ ဧ **499.5 499.5** Fiber-Optic Sensor Signal Displacement Sensor Signal Stop: Stop: Figure 3: Frequency Dependent Phase Shift in Fiber-Optic Signal:
A Comparison With the Signal of a Displacement Sensor
Located at the Beam Tip for 16 Hz. N Chan 00 Start: Start: Time O Rea1 200 ພ ພ > 800 500 \q p/ > E > E > E **E** -500 Real \d \tau \

Figure 4: Frequency Dependent Phase Shift in Fiber-Optic Signal:
A Comparison With the Signal of a Displacement Sensor
Located at the Beam Tip for 18.5 Hz.



s E S E 124.88 124.88 Displacement Sensor Signal **Stop:** Stop: Fiber-Optic Sensor Signal A Comparison With the Signal of a Displacement Sensor Located at the Beam Tip for 25 Hz. N **ഗ** ഗ Chan 0 0 Start: Time C Start: ω > Real 200 800 > E \d \d \d \d ਰ > > E > E `d i ∨ -800

Figure 5: Frequency Dependent Phase Shift in Fiber-Optic Signal:

8 8 62.439 Stop: Fiber-Optic Sensor Signal 0)

0

Start:

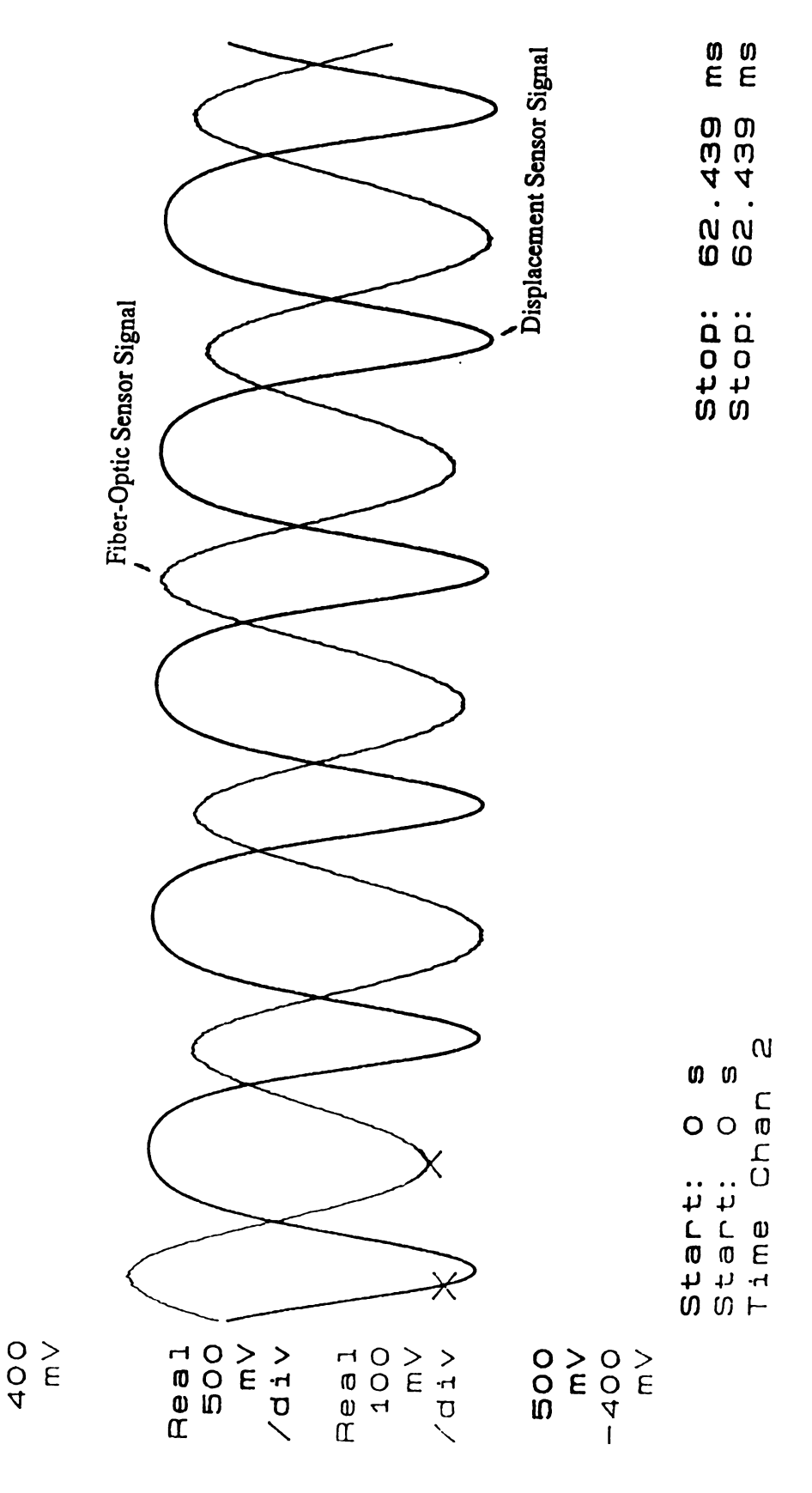
Figure 6: Frequency Dependent Phase Shift in Fiber-Optic Signal:
A Comparison With the Signal of a Displacement Sensor
Located at the Beam Tip for 55 Hz.

ω >

Displacement Sensor Signal 0 > 0 E ਜ > Real /d1/

Figure 7: Frequency Dependent Phase Shift in Fiber-Optic Signal:
A Comparison With the Signal of a Displacement Sensor
Located at the Beam Tip for 88.5 Hz.

4 ເບັ >



# E. Procedure for Imbedding Fiber-Optic Sensors in a Polymeric Composite Laminate

# E.1. Composite Manufacture Process

The composites used in the experiments described in this thesis were manufactured from AS4 3501-6 prepreg donated by Hercules Inc. This is a carbon-epoxy prepreg that was assembled by a hand lay-up method. The first specimens were laid up  $[(0/90)_3]_s$ , while other lay-ups used included  $[11_4/-11_4]_s$ ,  $[16_4/-16_4]_s$ , and  $[21_4/-21_4]_s$ . Here, the numbers within the brackets indicate the individual prepreg ply orientations within the laminate, the subscripts indicate the number of consecutive plys in a particular orientation, and the subscript s after the close bracket indicates that the plys within the bracket are repeated in reverse order in order to assemble a laminate that is symmetric about its midplane in the thickness direction.

The samples were assembled pending the curing process as shown in figure 8. The cork walls surrounding the prepreg laminate are present to prevent the flow of epoxy from the edges, which would result in a fiber volume fraction that varied with the distance from the edges of the plate. The purpose of the porous teflon is to allow the flow of epoxy from the laminate to the bleeder cloth without the cloth becoming attached to the composite. This allows an even distribution of the remaining epoxy across the cured laminate, although it will vary somewhat through the thickness of the laminate. The clear release film keeps the steel plates clean and unattached to the composite material.

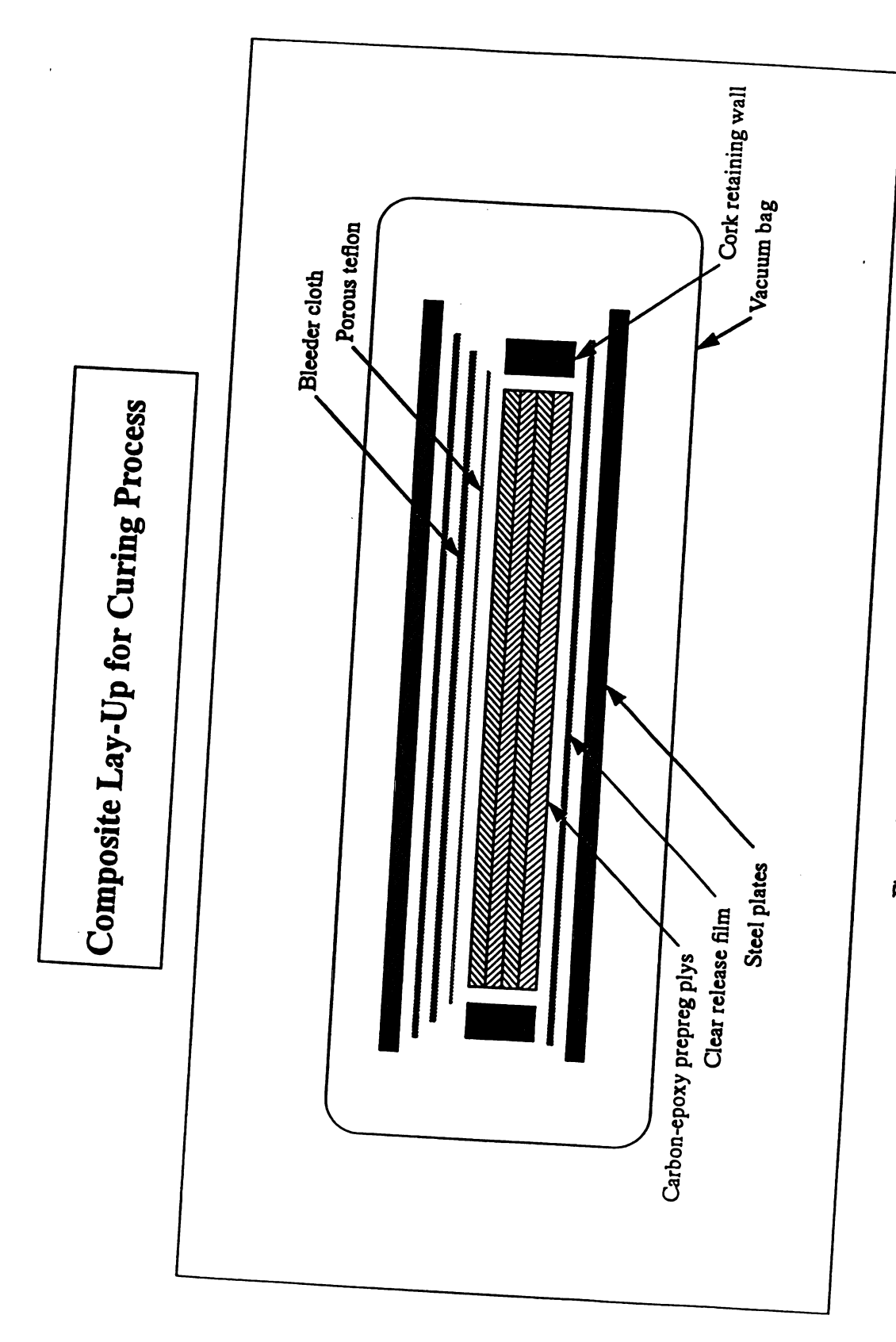


Figure 8: Composite Lay-Up for Curing Process

This assembly was then placed in a vacuum bag, which was evacuated and placed into a heat press. The heat press cured the composite plate at (240 F, 85 psi) for one hour after which the evacuation was stopped, and then at (350 F, 100 psi) for two more hours, as per the manufacturer's cure specifications. The cured composite was then allowed two to four hours to gradually lose pressure and cool to avoid damage due to thermal shock. The composite plate was then sectioned into beams using a diamond blade saw.

# E.2. Imbedding Fiber-Optic Sensors

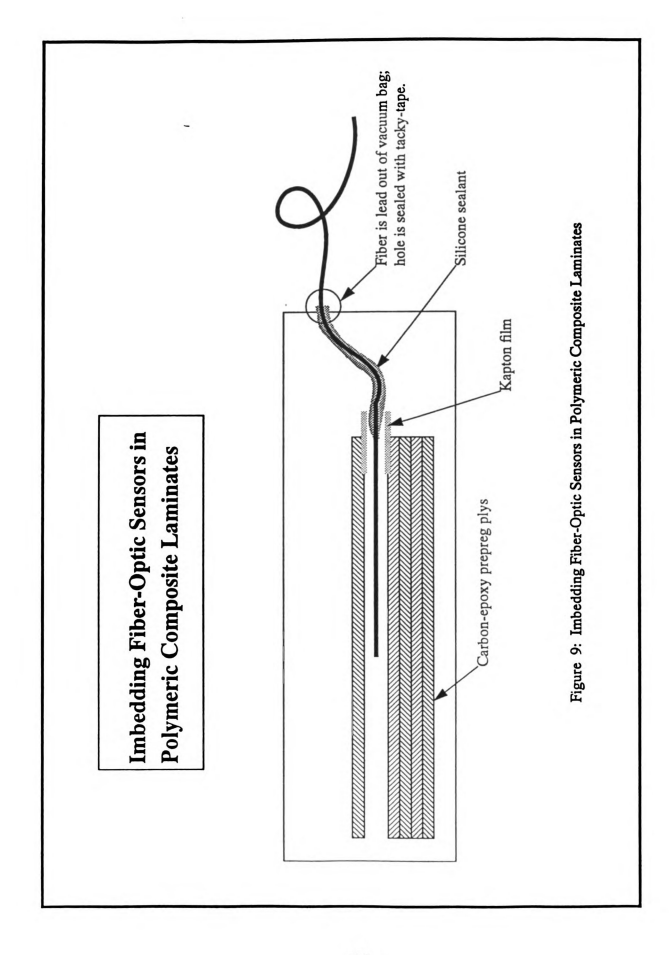
Care is required when imbedding fiber-optic sensors in a polymeric composite laminate because the fibers are apt to break, particularly where the fiber exits the composite. Also, a fiber coated by the matrix epoxy becomes brittle and prone to break.

Several steps were taken to protect the fibers. Two lead out methods were tried: in the first the fiber was lead out of the composite through a pinhole in the top ply of the laminate a few centimeters from the edge of the laminate, while in the second the fiber was lead directly out the edge of the laminate. The first method worked as long as the fiber-optic sensor was imbedded underneath the top one or two plys of the laminate only. Deeper positions resulted in sharper bends in the fiber, which resulted in the fiber being broken when exposed to cure pressures; a more gradual exit angle than a direct

normal to the laminate surface would alleviate this difficulty. The second method (leading the fiber strait out the edge of the composite) was preferred, since it introduced no unnecessary strains on the sensor during the cure of the composite. When the fiber was imbedded near the center of the composite plate (in the thickness direction) rather than the edge, a slice was made in the cork wall so the fiber would not have to bend around it. The slice was sealed with tacky tape to prevent the flow of epoxy through the rift. Most of the sensors were imbedded only one or two plys from the upper surface of the composite, however. This was to take advantage of the greater bend radius away from the neutral axis of the laminate, in order to maximize the strain on the fiber due to bending, so the sensor would be more sensitive.

The polymeric composite specimens were laid up  $[(0/90)_3]_s$ ,  $[11_4/-11_4]_s$ ,  $[16_4/-16_4]_s$ , and  $[21_4/-21_4]_s$ . The fiber-optic sensors were oriented in the zero degree direction in all these cases, so the direction of the sensor varied with respect to the direction of the carbon fibers in the prepreg plys adjacent to the sensor. The sensors functioned in each case. The sensitivity of each sensor varied so much with variables such as how well the laser light was coupled with the optical fiber, that it was difficult to ascertain what affect the orientation of the sensor with respect to the prepreg fiber angle had, if any.

Two further precautions taken to improve the survivability of the fiberoptic sensors are shown in figure 9. First, Kapton film was placed around the fiber for stress relief in the region where it exited the composite. Second, the



fiber of each sensor in a laminate was lead out an individual pinhole in the vacuum bag, leaving only to inches or so of fiber inside the vacuum bag but not within the laminate. The fibers were lead out individually, because when they were lead out a common hole, the leads inside the vacuum bag would lie on top of one another, and when cure pressures were applied the overlapping fibers broke each other. The exit pinholes were sealed with tacky tape to preserve the integrity of the vacuum bag. Finally, the portion of the fiber-optic sensor within the vacuum bag, but not within the laminate, was protected from embrittlement by the epoxy and other handling stresses by a coating of general purpose silicone sealant. This was accomplished by applying the silicone along approximately two inches of the fiber, starting from the end of the length of the sensor intending to be imbedded, and letting it cure. After the sensor was sandwiched between the plys of a laminate, the fiber leads were drawn out through a pinhole in the vacuum bag, before the vacuum bag was sealed. The fiber was drawn through until stopped by the silicone coated portion of the lead, and then the pinhole was sealed with tacky tape, which also held the fiber in position. Only then was the vacuum bag sealed and the cure begun. A carbon-epoxy composite plate made with imbedded fiber-optic sensors is shown in figure 10.

#### E.3. The Effect of Curing on the Fiber-Optic Sensor Performance

The length of fiber protected by the silicone showed some discoloration after the cure. The acrylate coating of the optical fiber turned brown due to the

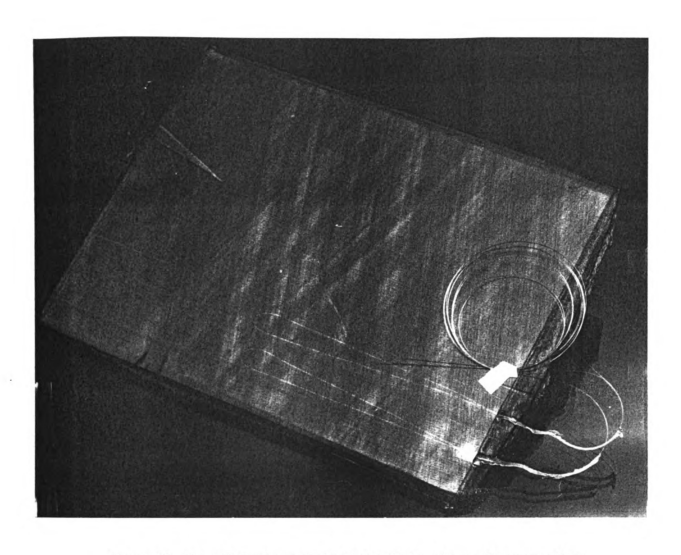


Figure 10: Fiber-Optic Sensor Imbedded in Carbon-Epoxy Composite Plate

heat present in the curing process. The only portion of the fibers thus affected was the length where the silicone sealant protecting the fiber was thin. Where the silicone coating surrounded the fiber there appeared no damage. The fiber within the composite material appeared unharmed as well. This was ascertained by removing a portion of one fiber from within the composite and observing it. This portion could be removed because the Kapton film prevented the bonding of the fiber to the composite roughly one centimeter in from the edge of the laminate. Although there was discoloration on some of the imbedded sensors, the sensors still functioned. This indicates that the core and cladding were undamaged, which is a reasonable result, since glass has a much higher melting temperature than the acrylate coating.

The signal strength of the imbedded fiber-optic sensor was less than its surface-bonded counterpart. Again, other variables such as the coupling efficiency affect this, but the cure process did seem to increase the attenuation of light passing through the sensor. Nevertheless, a signal sufficiently strong for the control algorithm to utilize was obtainable from an imbedded, single-ended, polarimetric fiber-optic sensor in a  $[11_4/-11_4]_s$  laid-up carbon-epoxy cantilevered beam (figure 11).

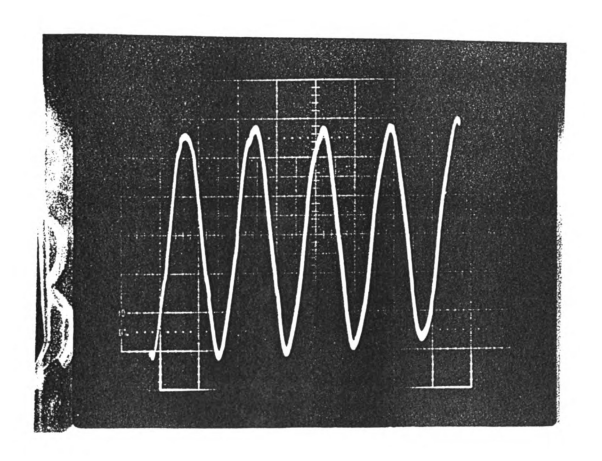


Figure 11: Imbedded Single-Ended Polarimetric Fiber-Optic Sensor Signal

#### F. Actuators

It is important in a smart structure that the actuators are an integral part of the structure itself. Rather than motors with moving parts, a smart structure actuator is a more reliable, no maintenance solid state material, preferably with low power requirements.

# F.1. Piezo-Electric Films and Ceramics

Piezo-electric materials produce an electrical charge when they are deformed, and conversely undergo a change in dimension when exposed to an electric field. This occurs because deformations change the volume of the material, and this results in a change in the net charge distribution within the film from the dipole properties of the film. The effect is a capacitive one, so induced charges will decay over time. In addition, the material is anisotropic, with the dipole alignment set by poling during the manufacture of the material.

There are two classes of piezoelectric materials: ceramics (such as BaTiO<sub>3</sub>) and polymeric films (polyvinylidene fluoride). The ceramics are stronger electromechanical transmitters than the films and can operate at higher temperatures, but they are also brittle and more massive. The advantages of the films are impressive: a dynamic range from 10<sup>-8</sup> to 10<sup>6</sup> psi, a frequency range from .005 to 10<sup>9</sup> Hz, a maximum voltage field of 75V/µm, and a voltage output (for sensing applications) an order of magnitude greater than the ceramic output for the same applied force. Also, the film is tough, flexible, lightweight, moisture insensitive, chemically inert, and inexpensive.

The stress-free ratio of strain developed to applied field is shown by the piezoelectric strain constant d. The form of this constant which is of greatest interest is d<sub>31</sub>, where the 3 indicates that the axis of the applied electrical field is in the thickness direction of the piezoelectric material, and the 1 identifies the axis of induced mechanical strain (or applied stress) as being in the length direction. For a piezoelectric film,  $d_{31}$  is approximately  $23x10^{-12}$  C/N, while  $d_{31}$ is  $78x10^{-12}$  C/N for BaTiO<sub>3</sub> piezoceramic, and  $110x10^{-12}$  C/N for PZT, a lead zirconate titanate piezoceramic. Thus, the amount of strain developed along the length of a beam with a piezoelectric actuator is d<sub>31</sub> times the field applied normal to the thickness of the beam. A ceramic produces greater strain than the film for the same applied field, however, the dielectric strength of the film (the dielectric strength is the maximum voltage per thickness that the material can stand without a breakdown in its piezoelectric properties) is 70 times greater than the dielectric strength of piezoceramics<sup>21</sup>.

Piezoelectric materials have been used extensively in the past in a variety of fields. Some devices exploiting the piezoelectric effect include sonar transmitters and receivers, robotic tactile sensors, switches, microphones, audio speakers, and fiber-optic modulators.

Both ceramic and polymeric piezoelectric materials can be used in a smart structure as sensors or actuators of strain. While ceramics have been imbedded in polymeric composites in experiments, their size and brittleness limits the strength and compliance of the structure they are incorporated in. Piezoelectric

films, on the other hand, are incapable of surviving the composite cure temperatures, but can be bonded between pre-cured laminates or can be surface bonded to a structure. Their presence has a much more benign influence on structures. Also, the use of a distributed actuator such as a piezo-electric film theoretically allows all modes to be controlled<sup>30</sup>.

# F.2. Electro-Rheological (ER) Fluids

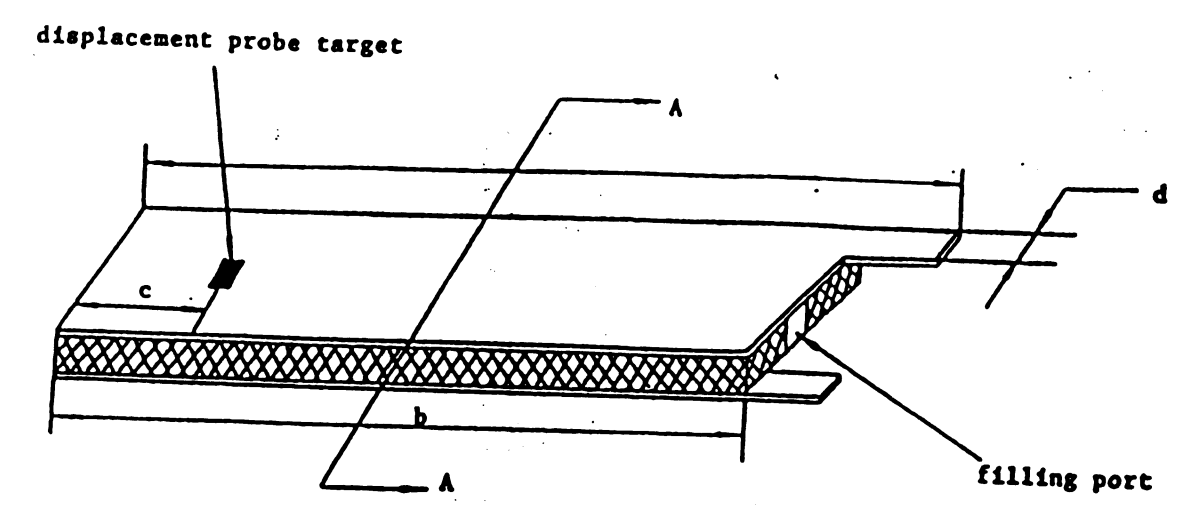
Electro-rheological fluids consist of polar particulates in a non-conductive suspension. The dipole associated with the particles may by inherent to the particle, as in a zeolitic ER fluid, or may be due to molecules of water which are bound to the particles, as in a starch based ER fluid. These particles have random positions and orientations within the suspension initially, but in the presence of a voltage field, the particles form chains as shown in figure 12. This results in a change in the viscosity of the fluid. Furthermore, the ER fluid can respond to voltage changes as rapid as 11 kHz<sup>25</sup>.

This effect is utilized by incorporating the ER fluid in a sandwich beam structure (see figure 13). The upper and lower plates act as electrodes, and so must be either made of a conductive material, or coated so as to be conductive. The rubber seal around the sides insulates the electrodes from one another so a voltage field may be applied and also serves to maintain the integrity of the structure, sealing in the ER fluid. Although voltages as high as 3-4 kV per mm between the electrodes are required, very little power is actually drawn because ER fluids are activated by a voltage field, so negligible current (about





Figure 12: Photomicrograph of ER Fluid at 0.0 kV/mm and at 2.0 kV/mm



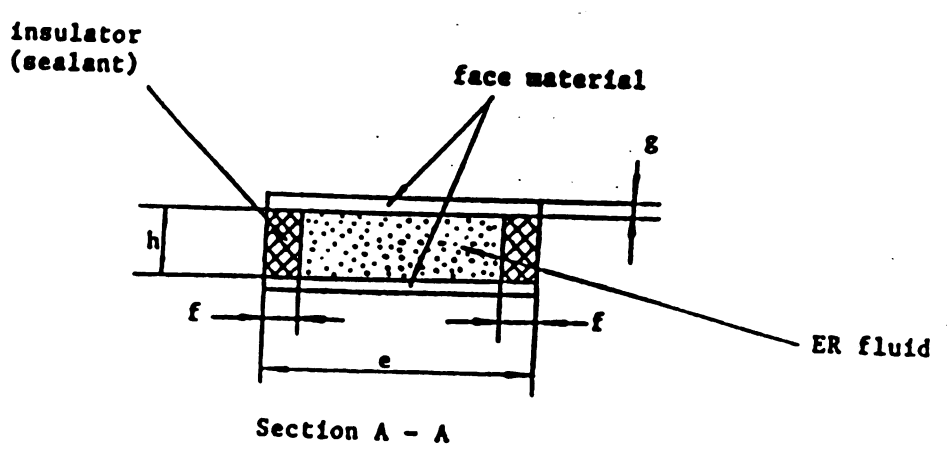


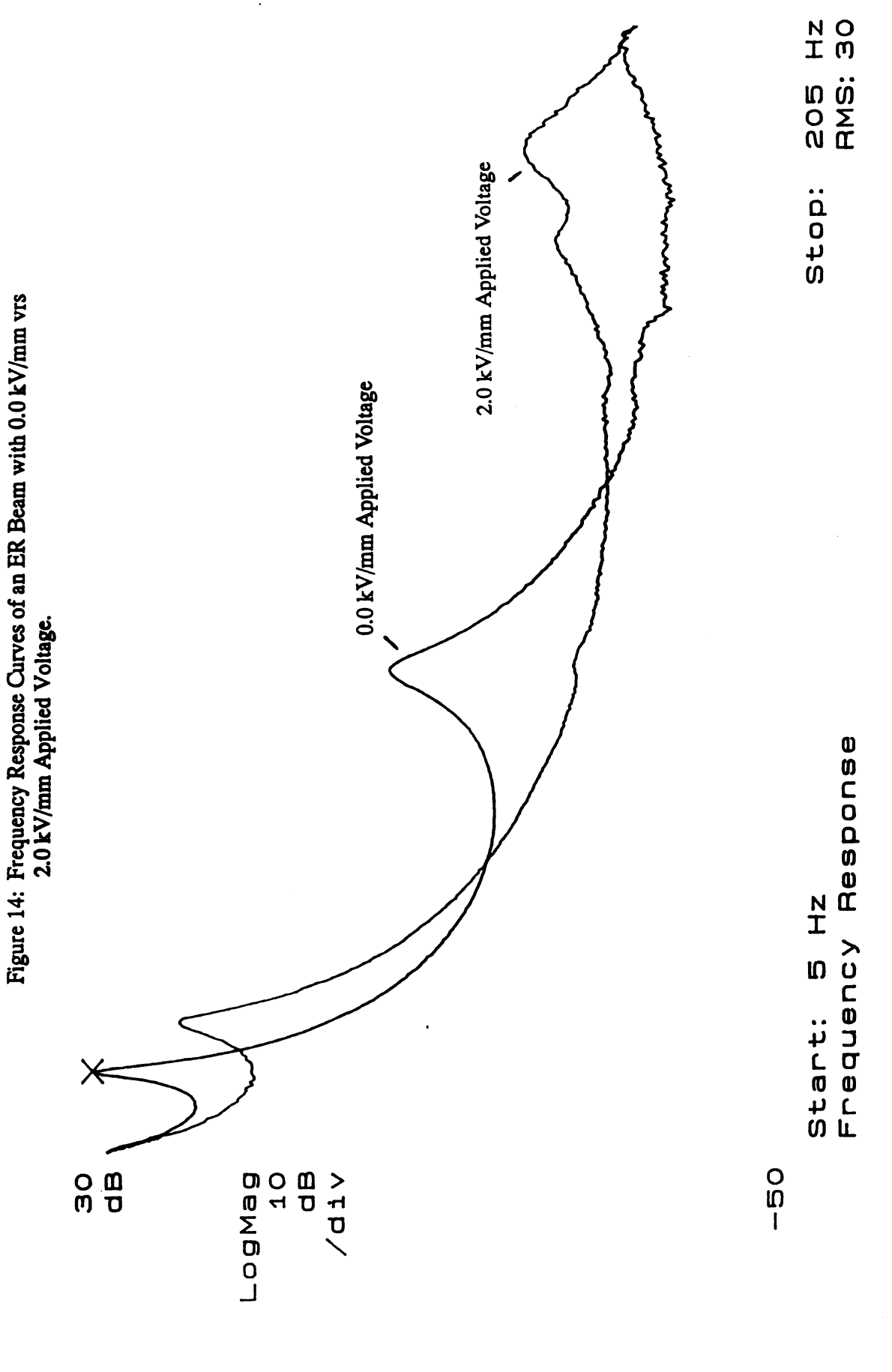
Figure 13: ER Fluid Sandwich Beam Structure

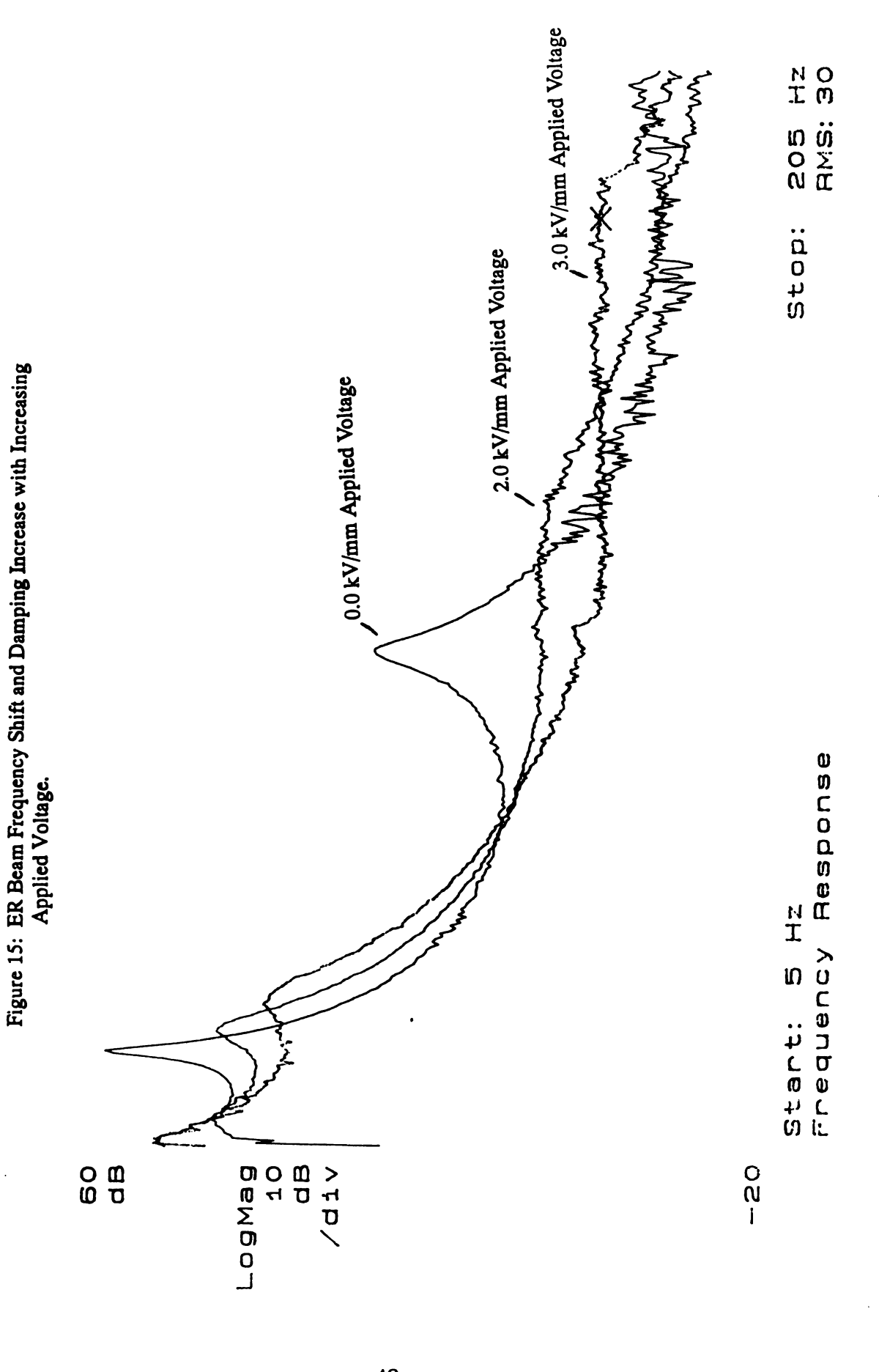
 $10 \,\mu\text{A/cm}^2$ ) flows between the electrodes.

In practice, when the beam is affixed in a cantilevered fashion, the activation of the ER fluid has two effects: the natural frequencies of the beam are raised due to the stiffening effect of the particulate chains, and the internal damping is increased due to the additional energy dissipation necessary to deform or break the chains. This is shown in figure 14. The magnitude of these two effects is dependant on the strength of the applied voltage field, up to a maximum achievable effect (figure 15). Both of these effects can be combined to reduce the amplitude of vibrations in the beam for a given applied excitation of the beam. The magnitude of the frequency shift is, however, dependant on the magnitude of the shear strain that the beam experiences. Larger shear strains exceed the yield stress of the chains, and when the chains are broken they have no stiffening effect. There is still a damping increase when the beam deformation is large because the chain structures continuously reform and energy is dissipated to break them. This vibration amplitude dependence for three voltage levels can be seen in the frequency response curves of figures 16-18.

# F.3. Shape Memory Metals, Magneto-Strictive Materials, and Other Potential Actuators

In addition to ER fluids and piezoelectric materials, potential classes of actuators for smart materials include shape-memory alloys and magneto-

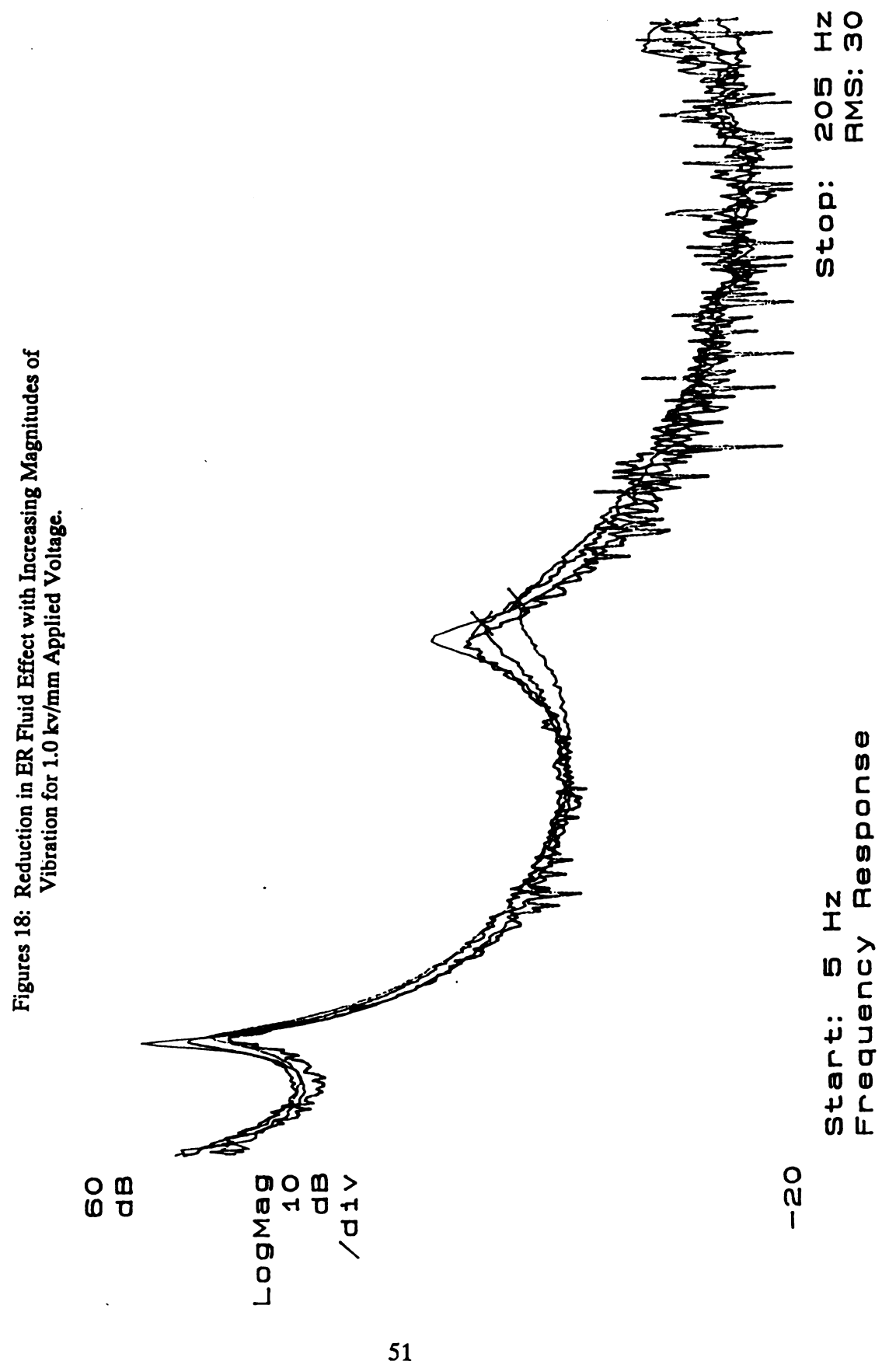




ROS HZ RMS: 30 Stop: Response NI Start: 5 F Frequency LogMag 10 10 db div В О О 0 1 8

Figures 17: Reduction in ER Fluid Effect with Increasing Magnitudes of Vibration for 2.0 kV/mm Applied Voltage.

50



strictive materials.

Shape memory metals can be trained to 'remember' a certain shape or configuration, such as a spring trained to remember an extended position, or a wire trained as a semicircular curve. When the device is heated beyond a preset critical temperature, it returns to its trained shape, regardless of how it has been deformed (up to strains as high as 8%<sup>31</sup>). Thus, the heated spring will expand to its remembered position, and the deformed wire will return to its curved configuration. Were similar wires to be incorporated in a composite structure, it would allow the structure to alter its shape or dimensions as required.

The earliest shape memory metals were NiTi alloys developed at the Naval Ordinance Laboratory in the 1960's, but since then better copper-based memory metals have been engineered. These metals may be heated by joule heating, or by external heating elements. Unfortunately, the response time of these materials is not fast enough for their use in active vibration reduction except for low frequency vibrations. Experimental work has been performed on low frequency vibration reduction in shape memory metal reinforced composite cantilevered beams<sup>23</sup> and in mode alteration by shape memory metals incorporated in composite panels for the purpose of noise reduction<sup>32</sup>.

Magneto-strictive materials are very much like piezo electric materials, except they change their dimensions when subjected to a magnetic field instead of a voltage field. Like piezo-electric ceramics, magneto-strictive

materials are brittle. Because they are so weak in tension, magneto-strictive actuators usually need to be operated in compression. When compressed the material is less susceptible to breakage and in addition produces significantly more output. The magneto-strictive material has an order of magnitude greater output than a piezoceramic material, up to approximately 2,000 parts per million<sup>29</sup>. Unfortunately, the hardware required to keep the actuator in compression detracts from its appeal for smart material applications.

More ductile alloys exhibiting magneto-strictive properties do exist, however, these are typically much weaker actuators.

Since magneto-strictive materials are activated by a magnetic field, the dangers of a high voltage field are eliminated. The magnetic field is typically induced by current passing through a wire coil around the actuator. The need for this coil is an additional drawback when considering magneto-strictive materials as potential smart actuators, especially in comparison to the simple, low-mass sputtered metal electrodes required by piezoelectric actuators.

### G. Control Algorithms

One of the requirements of a Class II smart material is the ability to send appropriate control signals to the actuators of the structure based on the input signals received from the sensors of the structure. This calls for a control algorithm, which is ultimately to be encoded on a single chip within the structure. For experimental research and development purposes, however, a programmable personal computer with digital-to-analog signal processing capabilities is more appropriate and versatile.

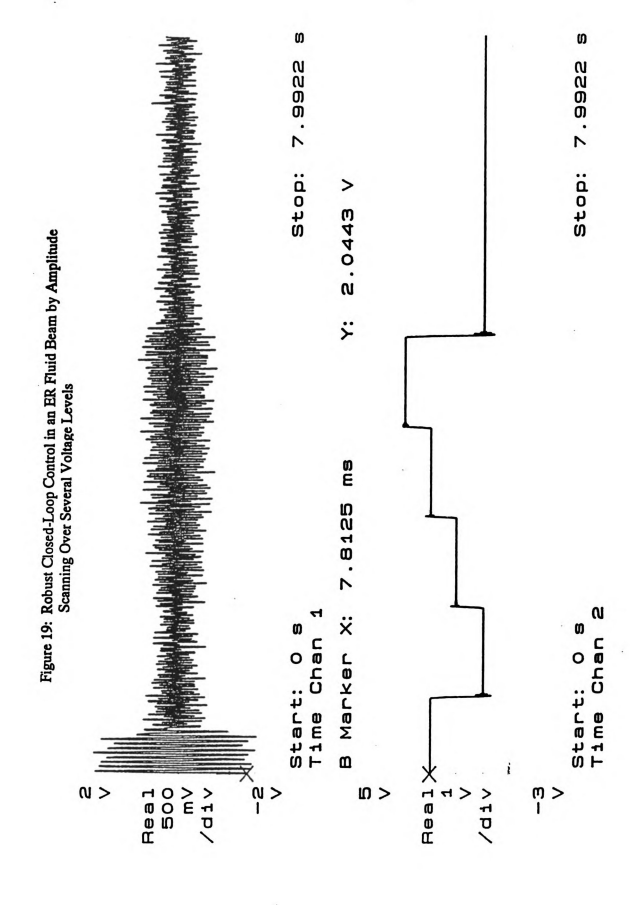
There are many possible control algorithms, from a look-up table approach to adaptive neural networks, and the advance of control intelligence is what will advance Class II smart materials into Class III smart materials once the imbedded actuator and sensor challenges are answered. The control method chosen will depend on the actual actuating system or systems present. In this thesis work, three control approaches were considered: two for use with beams with ER fluids and one for beams with piezoelectric actuators. These programs do not feature the most advanced control theories, but are adequately efficient for the demonstration of significant vibration reduction in smart structures.

The first method of control for ER fluid equipped beams uses a look-up table based on the frequency response curves of the beam at various voltages. The program calculates the frequency at which the beam is vibrating, and then applies the correct voltage, which results in the lowest amplitude of vibration at that particular frequency. If the excitation frequency shifts to a value where a different

voltage will reduce the magnitude of the vibration, the program will output that new voltage level. Thus, the bottommost curve of the various frequency response curves in figure 15 is followed. The program determines the correct voltage level to output for a given frequency by consulting a look-up table. Each particular beam must be characterized by specific frequency response curves at various voltage levels in order to set the correct values in the look-up table in the program for that beam.

The second control program for ER fluid equipped beams is a more robust version of the first in that the beam need not be characterized nor the program adjusted prior to its use. This program scans the beam by applying different voltage levels in steps from zero to a specified maximum voltage and finds the voltage at which the vibrational amplitude of the beam is at a minimum. It keeps that voltage level applied until a change in the amplitude is detected, corresponding to a change in the forcing parameters, whereupon it initiates the scanning sequence again (see figure 19). Although this program will minimize the vibration levels in a beam of unknown characteristics, it does not reduce vibrations as quickly as the first control program when the forcing frequency is altered because the scan sequence requires a finite amount of time at each voltage increment for the beam to respond, so that an accurate assessment of the optimal voltage level for minimum vibration amplitudes may be found.

A different control method is necessary for beams equipped with piezoelectric actuators. These beams do not reduce vibrations by shifting the



natural frequencies of the beam away from the excitation frequency as ER fluid equipped beams do, but rather reduce vibration by forcing the beam in opposition to the perturbing force. This requires an algorithm that will have the piezoelectric film (or ceramic) actuate at the same frequency as the sensed excitation frequency but out of phase with the beam velocity.

This algorithm does not work well with distributed polarimetric fiber-optic sensors because of the frequency dependent phase shift associated with them. Possibly a look-up table and output delay loop could be used to correct for the lag, but this is a cumbersome solution. In the case where the polarimetric fiber-optic sensor has a sensing length such that the signal is close to 180 degrees opposed to the velocity signal at the fundamental frequency, then this closed-loop control can dramatically reduce forced vibrations at this resonance. Note, however, that this frequency dependant phase shift is of no concern for the control of ER fluid equipped beams where phase information is not required, only the frequency. It is also important to point out that the fiber-optic sensors need no insulation from the high voltage fields present in ER beams because the optical fibers do not conduct electricity. Therefore, no special precautions need to be taken to protect the sensing and signal processing equipment, which is not the case for strain gauges and most other conventional sensors.

### H. Experimental Program

# H.1. Goals

The experimental program goals included the development and comparison of interferometric and polarimetric fiber-optic sensors (including single-ended leads and imbedded variations), the assembly and characterization of ER fluid and piezoelectric actuator equipped beams, and the integration of the above sensors and actuators with control algorithms for the purpose of vibration reduction in prototype Class II smart materials.

## H.2. Experimental Procedures

The configurations of the various sensors on cantilevered beams are shown in figure 20, while the optical set-ups for the interferometric and polarimetric fiber-optic sensors are shown in figures 21 and 22, respectively. Note in figure 20 that the Mach-Zehnder interferometer has two fiber loops bonded to the beam. The shorter loop is the reference arm of the interferometer. It is positioned adjacent to the sensing arm in order that the leads both experience the same perturbations. This makes the leads insensitive, leaving only the additional length of the sensing arm sensitive to strain. For this reason, this configuration was chosen over the separate arm configuration of figure 21. To integrate the strain over a length instead of only at a point, it is only necessary to increase the length of the sensing loop with respect to the reference loop, up to the limit imposed by the coherence length of the laser (typically on the order of 25 cm for HeNe lasers).

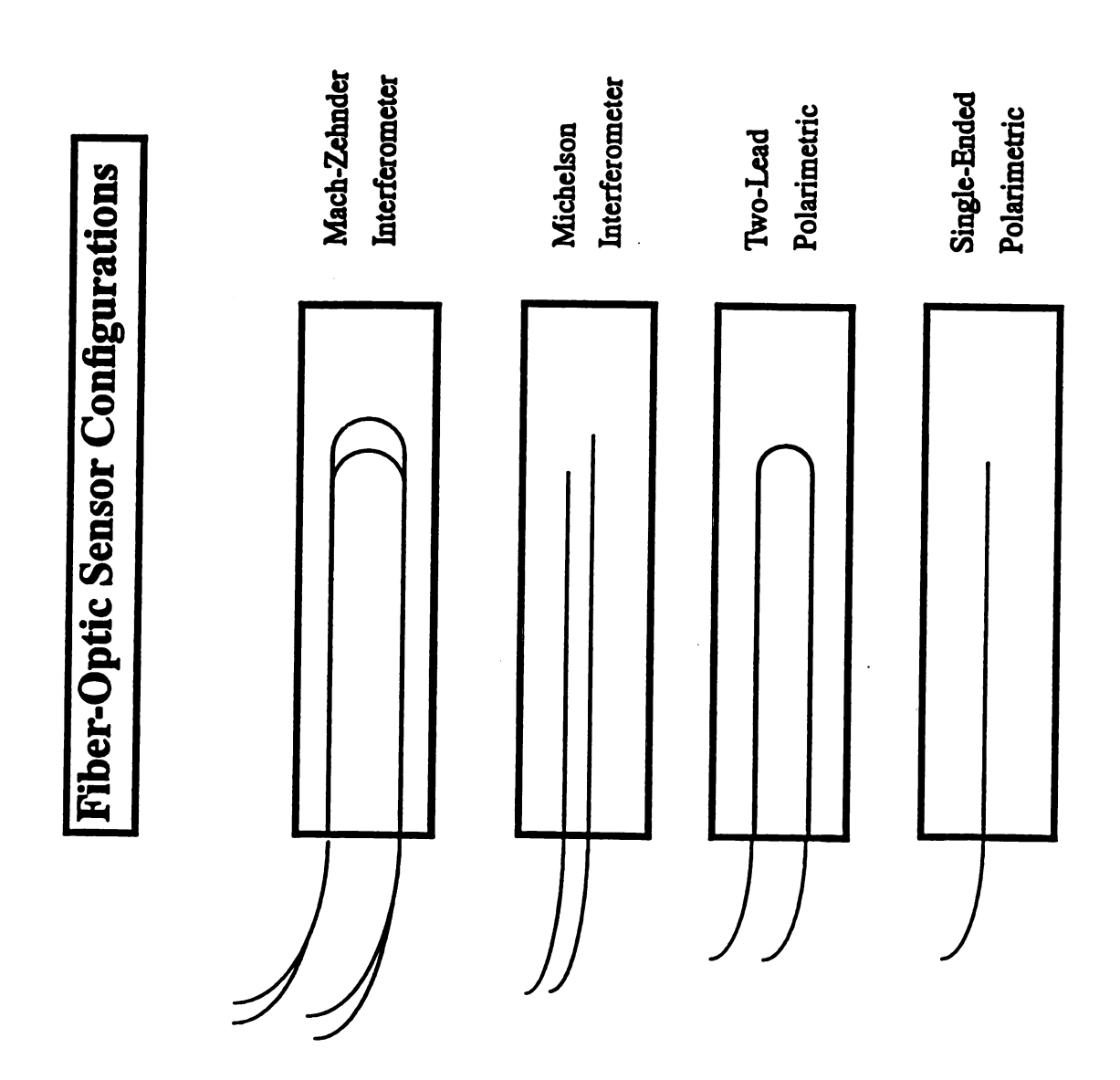


Figure 20: Fiber-Optic Sensor Configurations

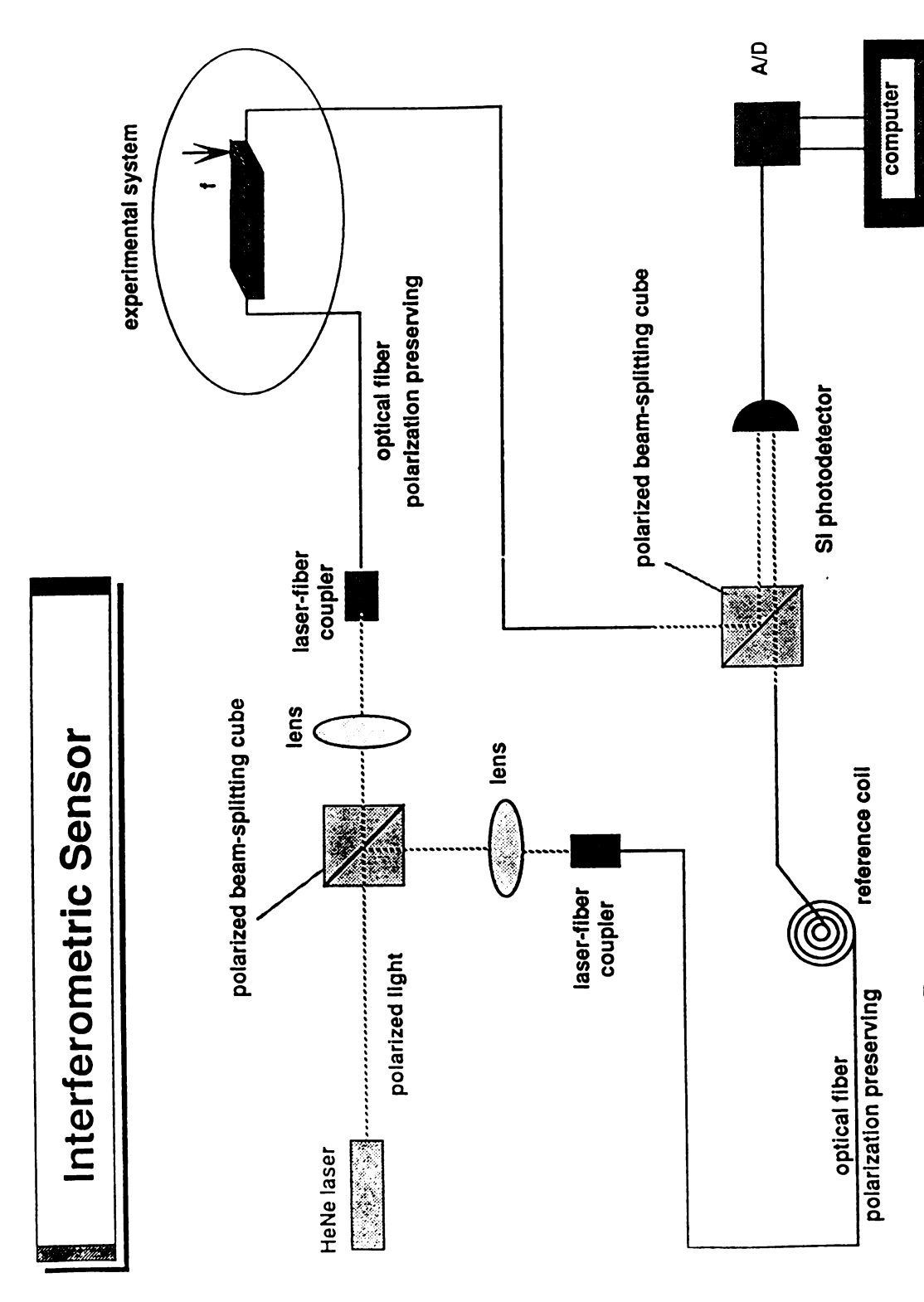


Figure 21: Mach-Zehnder Interferometric Fiber-Optic Sensor Optical Set-Up.

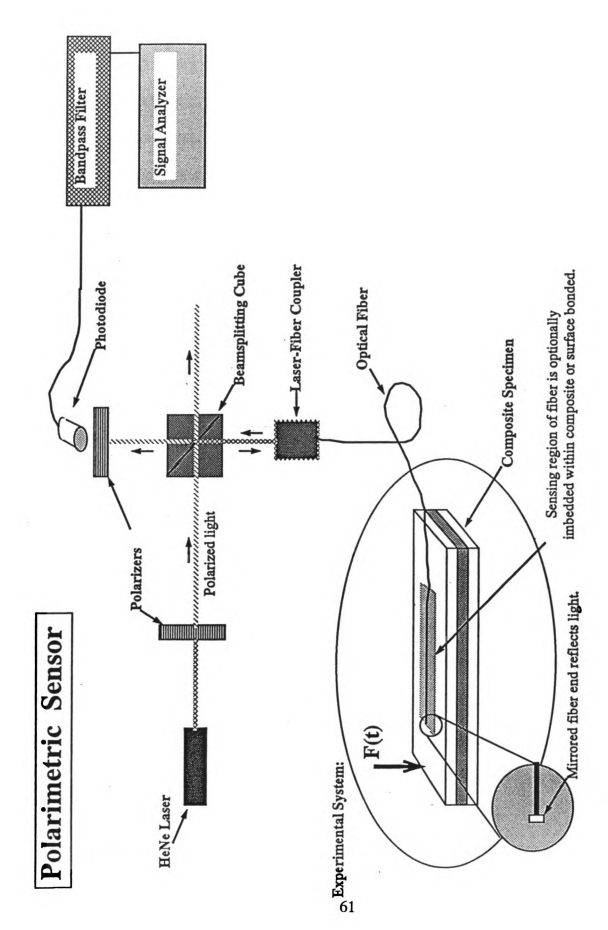


Figure 22: Polarimetric Fiber-Optic Sensor Optical Set-Up

A variety of optical fibers were used in manufacturing the various sensors, but Corning Flexcor single-mode fiber #50633.126 with CPC3 coating was used more than any other kind of fiber. The CPC3 coating is an acrylate coating with a 250 µm outer diameter. The acrylate coating does not withstand cure temperatures as well as special polyimide coatings, but it was found that the sensors with the acrylate coating imbedded within carbon-epoxy laminae still functioned adequately after undergoing the cure process.

None of the imbedded sensors survived the cure process intact before the protective measures described previously were taken. Of the fibers imbedded with protective measures, roughly 75% were functional. The dysfunctional fibers were for the most part those fibers exhibiting coating damage due to an incomplete coating of silicone sealant.

To ensure coherence in the interferometric sensors, light from a single Helium-Neon laser source is split via a beam-splitting cube into two beams with (nearly) half the power each of the source beam. The light is coupled into the single-mode optical fiber arms of the interferometer using two Newport M-F-1015 Precision Single Mode Fiber Couplers. The light emitted from the exiting end of the two fibers is recombined using a second beam-splitting cube. The ends of the fibers must be aligned in order to obtain the optical fringes formed by the interference of the two exit beams. The fringe pattern falls on a slit in front of photodiode, so that an impulse signal is obtained as each bright fringe shifts across the face of the slit. To improve the strength of this signal, a

63

multiple slit filter was manufactured to cover the face of the photodiode and positioned so that fringes of the same kind were aligned with each slit of the multiple slit array (see figure 2). Thus, as the fringes shift, several bright fringes align with the slits and shine onto the photodiode instead of only one. This results in a signal similar to the one in figure 23.

As an improvement on this sensor, a Michelson interferometric sensor was developed by silvering the ends of the fibers used as the arms of the interferometer. This reduced the complexity of the sensor in three ways. First, only two leads into the sensing region are required, so the amount of fiber needed is reduced, the potential for breakage is lowered, and there is less intrusion to the structure. Second, no loops are now required for the leads to enter the beam from the same end, so the required width of the sensor is drastically reduced, and there is no more light loss due to the bend. Third, the reflected light exits out the same apparatus which originally coupled it through the fourth side of the beam-splitting cube; and so the alignment for obtaining fringes is automatically accomplished, and one less beam-splitting cube is needed.

When the Michelson sensor was surface-bonded to a cantilevered beam, three fibers were positioned with different lengths. This was to allow any two of the leads to be used as a Michelson interferometer, in case any one of the leads was defective in some way. If all three leads worked properly, then the three different combinations would allow for comparisons of fringe patterns and sensor sensitivity between sensors with different sensing lengths.

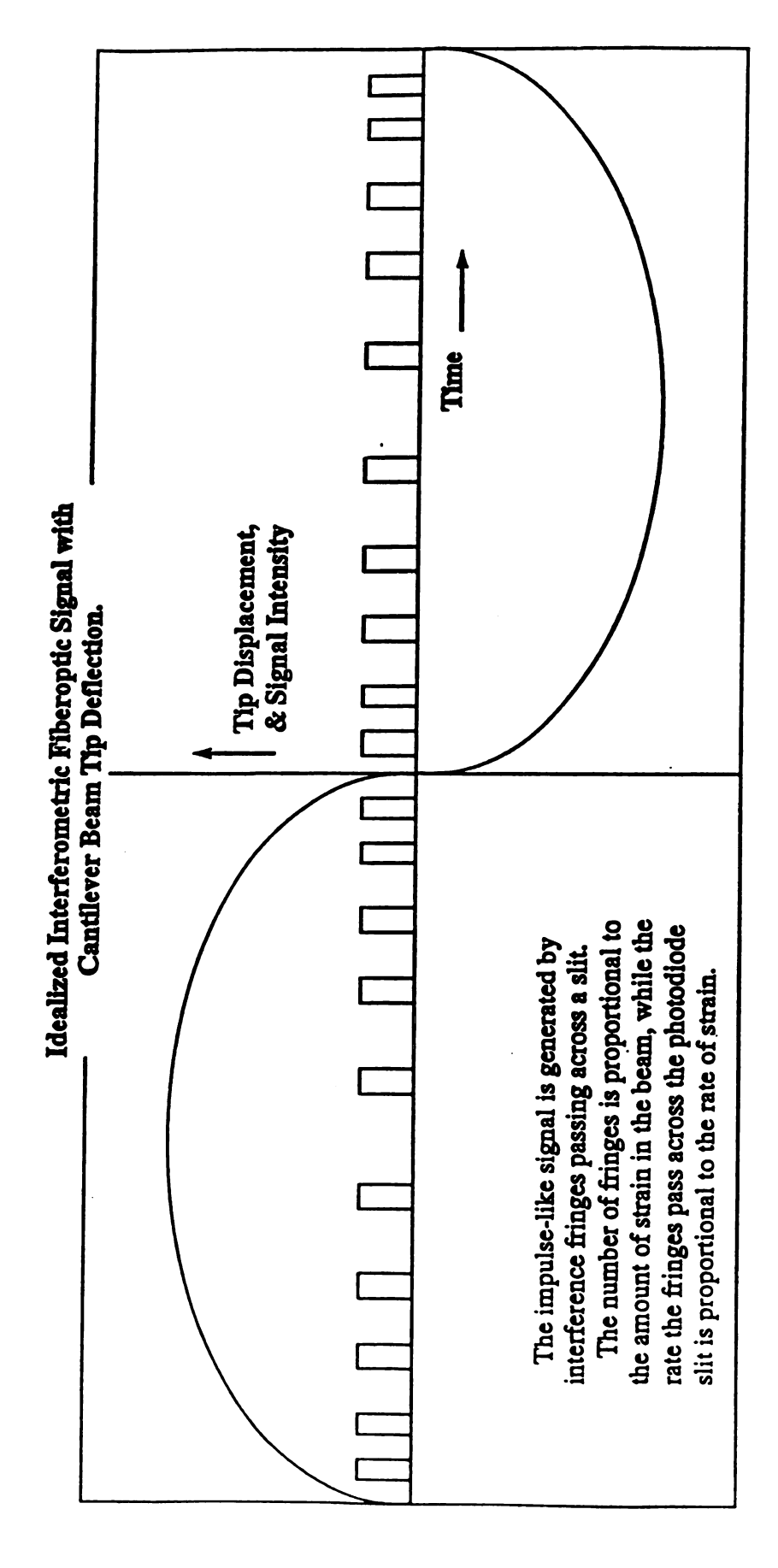


Figure 23: Idealized Interferometric Fiber-Optic Signal with Cantilever Beam Tip Deflection.

65

Both of the above interferometric sensors produced fringes, and with the aforementioned slitted photodiode discernible signals were received. For the purpose of real-time control of vibrations, however, the signals produced by the interferometric sensors were not readily useful. The number of fringes passing by a slit is proportional to the magnitude of the strain, while the rate at which the fringes pass is proportional to the rate of strain. A control program would need to find the beginning and end of a cycle from the relative spacing between the fringes, then calculate the frequency from the number of fringes in the cycle and the length of time of the cycle. Unfortunately, this spacing varies with strain and rate of strain. This would be a difficult task to accomplish in real-time.

In contrast, the signal from a polarimetric fiber-optic sensor is a sinusoidal response with the same frequency as the forcing frequency, resulting in a signal easily used by control algorithms. The polarimetric sensor, although less sensitive than the interferometric sensor, did produce a signal sufficiently clear for use. For these two reasons, the research into interferometric fiber-optic sensors for vibrational control purposes was dropped in favor of polarimetric fiber-optic sensors. Figure 24 shows one carbon-epoxy composite beam with two surface-bonded single-ended polarimetric fiber-optic sensors (top), and two carbon-epoxy composite beams with imbedded single-ended polarimetric fiber-optic sensors. All surface-bonded fiber-optic sensors were attached to aluminium or carbon-epoxy composite beams using a commercial superglue.

Beams with piezo-electric film actuators were assembled by adhering the

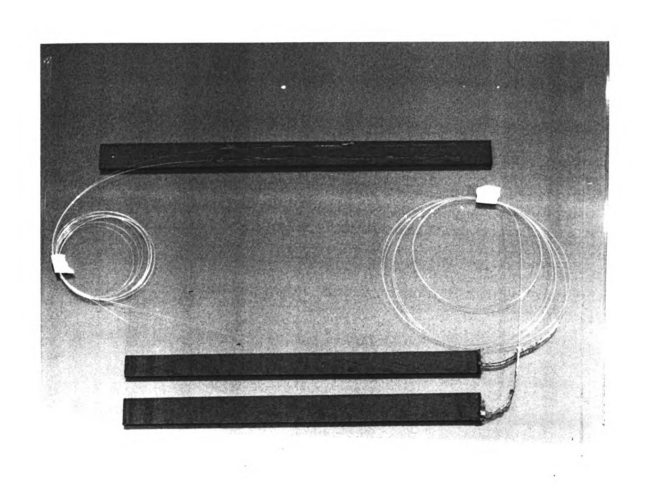


Figure 24: Surface- Bonded and Imbedded Fiber-Optic Sensor Equipped Carbon-Epoxy Composite Beams.

actuators to the beam with a commercial superglue. The silvered portions of the actuators were 15.5 cm long, not counting the leads, and 19 mm wide, but the film itself was 1.5 mm wider along each side than the electrodes. Each actuator was positioned so that the end with the leads was approximately one centimeter from where the clamp held each beam. Piezo-electric actuators were used on both aluminum beams and carbon-epoxy composite beams. These beams, as well as the ER fluid beams, were insulated from the clamping fixture to avoid grounding high voltages into the Ling Dynamic Shaker.

Both hydrophilic and hydrophobic electro-rheological fluids were mixed for incorporation into beams. A variety of particulate to fluid mass rations were mixed in each case. Although both varieties exhibited changes in viscosity with voltage, those beams incorporating hydrophilic ER fluids exhibited superior breadths of performance, and the results presented in this thesis are from hydrophilic ER fluid beams only.

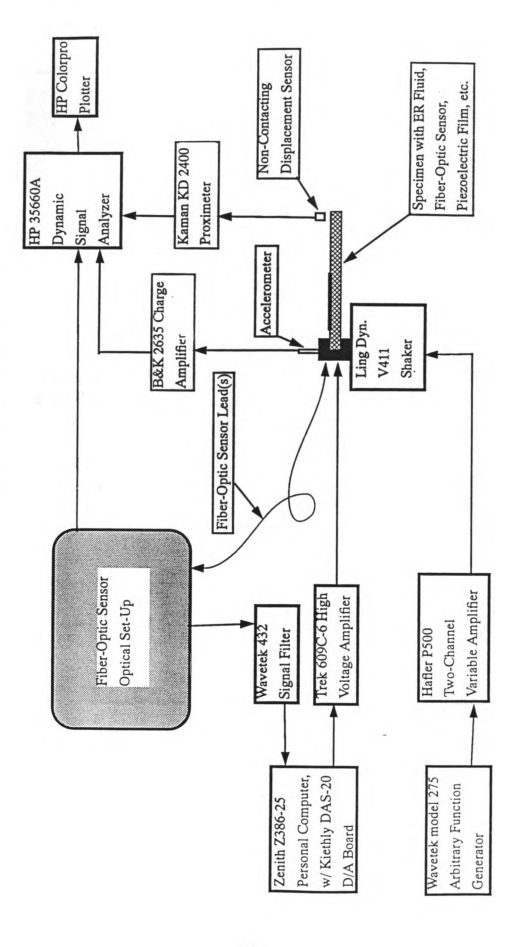
The beams containing electro-rheological fluids consist of the fluid, contained by a rubber seal sandwiched between two plates (fig 13). The plates act as electrodes and must either be made of a conductive material or coated with one. The beams used in this work had aluminum plates, although carbon-epoxy composite plate beams had been investigated in previous studies as well. The beams were assembled using RTV silicone for the sealant. This manufacturing of ER beams follows the procedures described by Gandhi, Thompson, and Choi in reference 25.

The optical experimental set-up for the polarimetric sensor equipped smart beam is shown in figure 22, and the rest of the equipment is shown in figure 25 and pictured in figure 26. The ER fluid or piezo-electric film equipped cantilevered beam is excited by the Ling Dynamic V411 Shaker, which is controlled through a Hafler P500 Variable Amplifier by a Wavetek Model 275 Arbitrary Function Generator. The strain in the beam is coupled to the fiber sensor. From the optical set-up, the photodiode signal is conditioned by a Wavetek 432 Signal Filter and then converted into a digital signal by a Keithley DAS-20 D/A Board as input for one of the control algorithms run on a Zenith Z386-25 Personal Computer. The program control signal is converted by the Keithley board and Amplified by a Trek 609C-6 Voltage Amplifier on the way to activating the ER fluid or piezo-electric film to reduce vibrations in the beam. An accelerometer signal conditioned by a B&K 2635 Charge Amplifier and a displacement signal from a non-contacting Kaman KD-2400 Proximator are lead to a Hewlett-Packard 35660A Dynamic Signal Analyzer for comparison with the fiber-optic sensor signal. These two sensors are also used with the signal analyzer to obtain the frequency response curves required by the look-up table control program. The results are plotted using the HP Colorpro Plotter.

# H.3. Results and Accomplishments

Throughout the experiments, several interesting phenomena were observed. One of these is the frequency dependant phase shift in the

Figure 25: Smart Structure Experimental Set-up



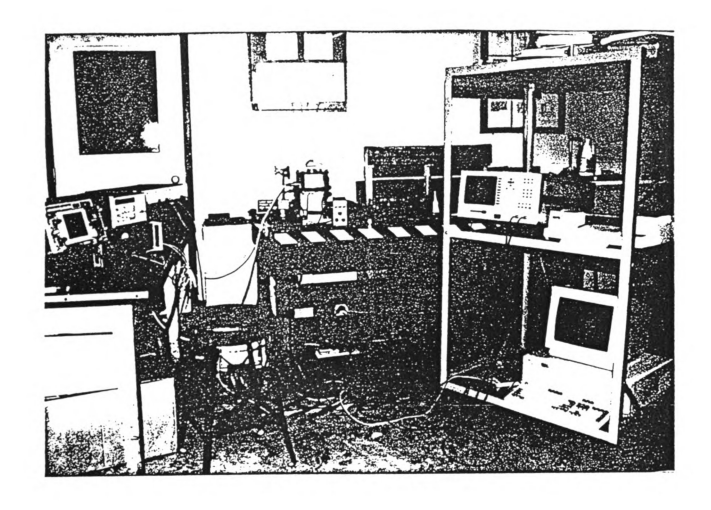


Figure 26: Photograph of Smart Structure Experimental Apparatus.

polarimetric fiber-optic sensor signal mentioned previously, and documented in figures 3-7. Discussed earlier are the characteristics of an ER fluid equipped beam. The beams experience an increase in their damping factor and a shift in their natural frequencies when voltage is applied to the fluid (see figure 14) as the voltage causes the suspended particles to align in chains (fig 12). Furthermore, as shown in figures 16-18, the shift in the natural frequencies of the beam with applied voltage is reduced by large shear strains. Large strains in the beam break the particulate chains of the ER fluid resulting in the negation of the stiffening effect of the fluid on the beam. The damping, though, remains higher in an activated beam even when large strains are present because of the additional energy loss required to continuously break the particulate chains.

In figures 27 and 28 the signal from a single-ended surface-bonded polarimetric fiber-optic sensor is compared with the displacement signal from a non-contacting displacement sensor located at the tip of a 19.5 cm long cantilevered carbon-epoxy composite beam which is being forced at its first fundamental natural frequency (41.2 Hz) with a tip displacement of 1 mm. In the first figure, the Wavetek model 432 Signal Filter only acts as a DC cut-off and signal gain. While in the second figure, the filter low-pass is set to 110 Hz. The improvement in the signal arises from the elimination of the noise from the overhead lights, which operate at 120 Hz. This source of noise results from the use of bulk optics in the experiment. The use of bulk beam splitters,

ຫ E ຮ **E 62.439** 62.439 Fiber-Optic Signal Stop: Stop: Figure 27: Comparison of Single-Ended Polarimetric Fiber-Optic Sensor Signal with Non-Contacting Displacement Sensor at Beam Tip Displacement Sensor for Small Excitation Amplitudes at Resonance (41.2 Hz) 0 Chan Start: Time C Start: 1 0 E 0 > 0 > 4 0 E 0 > π εου τοοΕ ο Ο Ε 100 E \d; \c/ 4 > /d1/ Real

8 E 8 E 62.439 62.439 Stop: Stop: Fiber-Optic Signal Figure 28: Same as Figure 27, but Low-Pass on a Bandpass Filter Set to 110 Hz to Filter Noise from 120 Hz Overhead Lights Displacement Sensor Chan Start: Time C Start: 0 E S 4 > > 0 > 100 **>** /41/ 1400 Real

couplers, etc., is convenient for laboratory use where a variety of optical configurations are examined, but in practice these elements in smart structures would be replaced by all fiber couplers, pigtailed sources, etc. Thus ambient light noise terms will not be problematic in applied fiber-optic sensor systems. When the polarimetric fiber-optic sensor signal strength is small, due to very small vibrations, inadequate coupling of light to the fiber, or other reasons, the 60 Hz line noise in the support hardware can become significant enough to warrant filtering out as well.

To show an alternative use for the polarimetric signal, the HP 35660A Signal Analyzer was used to determine the frequency response curve of a carbon-epoxy composite cantilevered beam using first a conventional non-contacting displacement sensor located at the tip of the beam and then the signal from a polarimetric fiber-optic sensor. The two results are shown in figure 29. The vertical displacement of the fiber-optic sensor signal is an indication that the relative strength of the signal is less than the proximeter signal strength. The proximeter signal strength is a function of its proximity to the vibrating surface and of the reflectivety of the surface, and so it is limited to a location where the vibrating surface will not strike the proximeter but close enough for a clear signal. The polarimetric fiber-optic sensor, on the other hand, is located on or within the vibrating surface and so need not be repositioned each time the magnitude of the vibration changes. The figure clearly shows that the results using the fiber-optic sensor are as informative as the results using the displacement sensor.

Figure 29: Comparison of Frequency Response Curves Generated Using Proximeter and Polarimetric Fiber-Optic Sensor Signals.

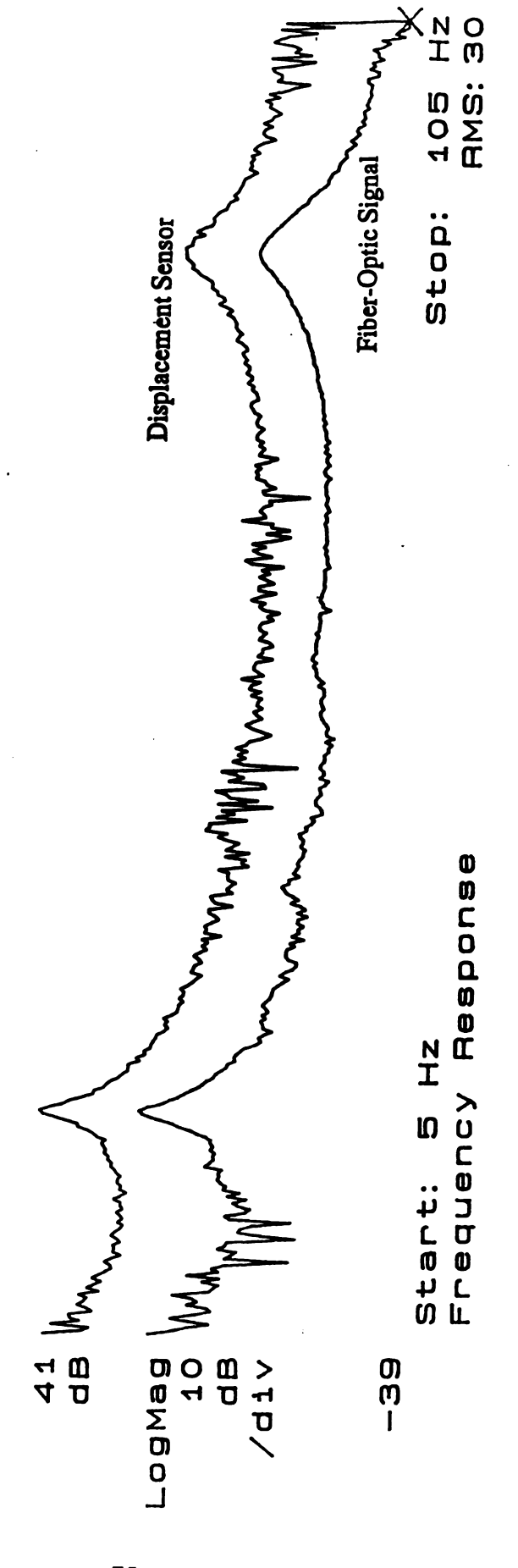


Figure 30 is a photograph showing the beam tip velocity signal and the phase-based control algorithm output in response to the signal. This control is a 'bang-bang' actuation, where the actuator (in this case a piezo-electric polymeric film) forces the beam it is bonded to in opposition to the actual vibrational mode of the beam in order to reduce the magnitude of the vibration of the beam. As mentioned previously, the phase relation between the polarimetric fiber-optic sensor signal and the tip deflection varies depending on the length of the sensor and the frequency of vibration. When this length is adjusted so that it is nearly 180 degrees out of phase with the tip velocity of the beam when the beam is excited at its fundamental frequency, the polarimetric fiber-optic sensor can then be used for piezo-electric actuator control of first mode forced vibrations, which are the most necessary to control in cantilevered beams. As shown in figure 31, the magnitude of the forced vibration is reduced by a factor of five using this method. The piezo-electric film was operated at 750 V, well below its maximum operating voltage of 2 kV.

Scanning control of beams incorporating electro-rheological fluids works on beams of unknown frequency characteristics by applying different voltage levels long enough to ascertain whether the magnitude of vibrations is improving or worsening in comparison with the other voltage levels, and then settling on the best available voltage level until conditions worsen (due to a change in the excitation frequency, for example). This is shown working in figure 19.

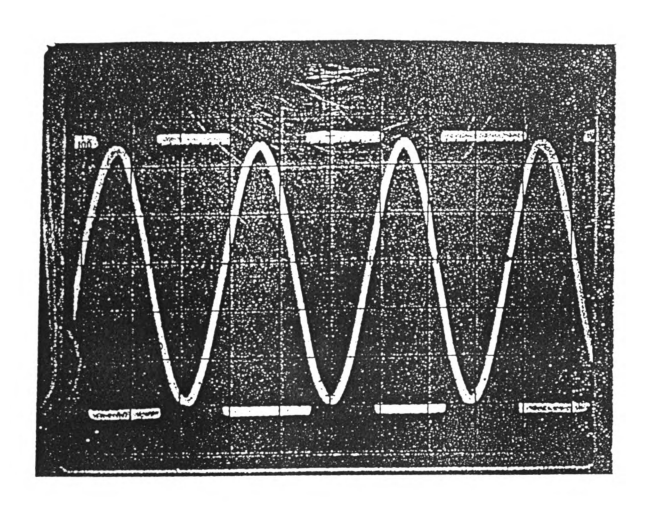
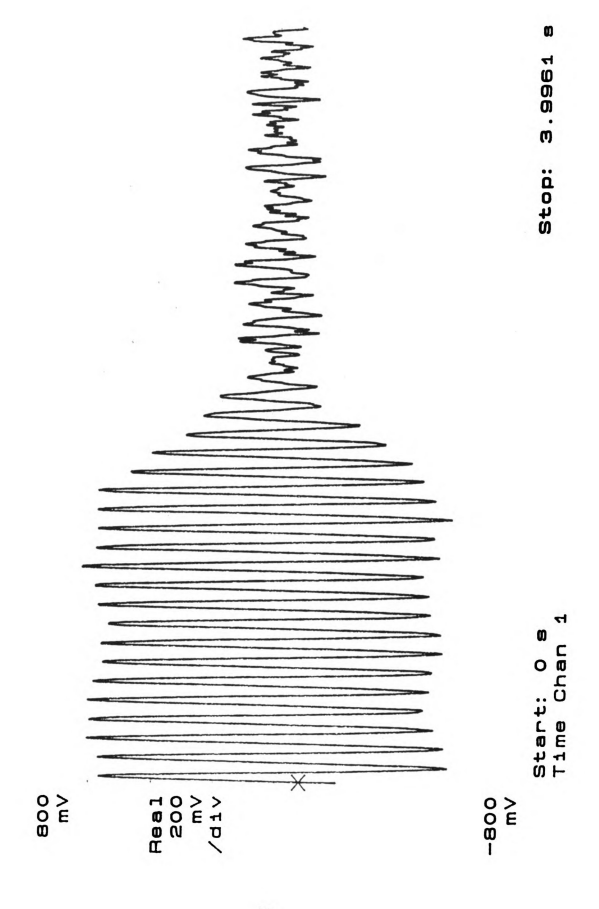


Figure 30: Phase-Based Control Algorithm Response to Tip Velocity Signal.

Figure 31: Forced Response as Phase-Based Closed-Loop Control Begins.



78

Better control is possible when beam characteristics are known, through the use of a look-up table control approach. The frequency response curves in figure 14 show the change in the magnitude of the vibration of the beam with the change in the forcing frequency for an ER beam at 0.0 kV/mm and the same beam at 2.0 kV/mm. From the figure, it can be seen that the vibration will be less when the voltage is at 2.0 kV/mm when the forcing frequency is less than 24 Hz, but between 24 Hz and 124 Hz the magnitude is less with 0.0 kV/mm, and so on. Intermediate voltage levels can lower the vibration magnitude at narrow frequency bands (as evident from figure 15) but compared to the 'on/off' method any improvements are only incremental.

The results of using the look-up table approach with ER fluid equipped beams are presented in bar graph form in figure 32. This figure compares the response of the beam with no applied voltage, constant gain voltage, and closed-loop control using polarimetric fiber-optic sensors and, for comparison, a non-contacting displacement sensor. The closed loop reduces the vibration magnitude on the constant applied voltage by over 50% at some frequencies and reduces the vibration magnitude over no applied voltage by over 95%.

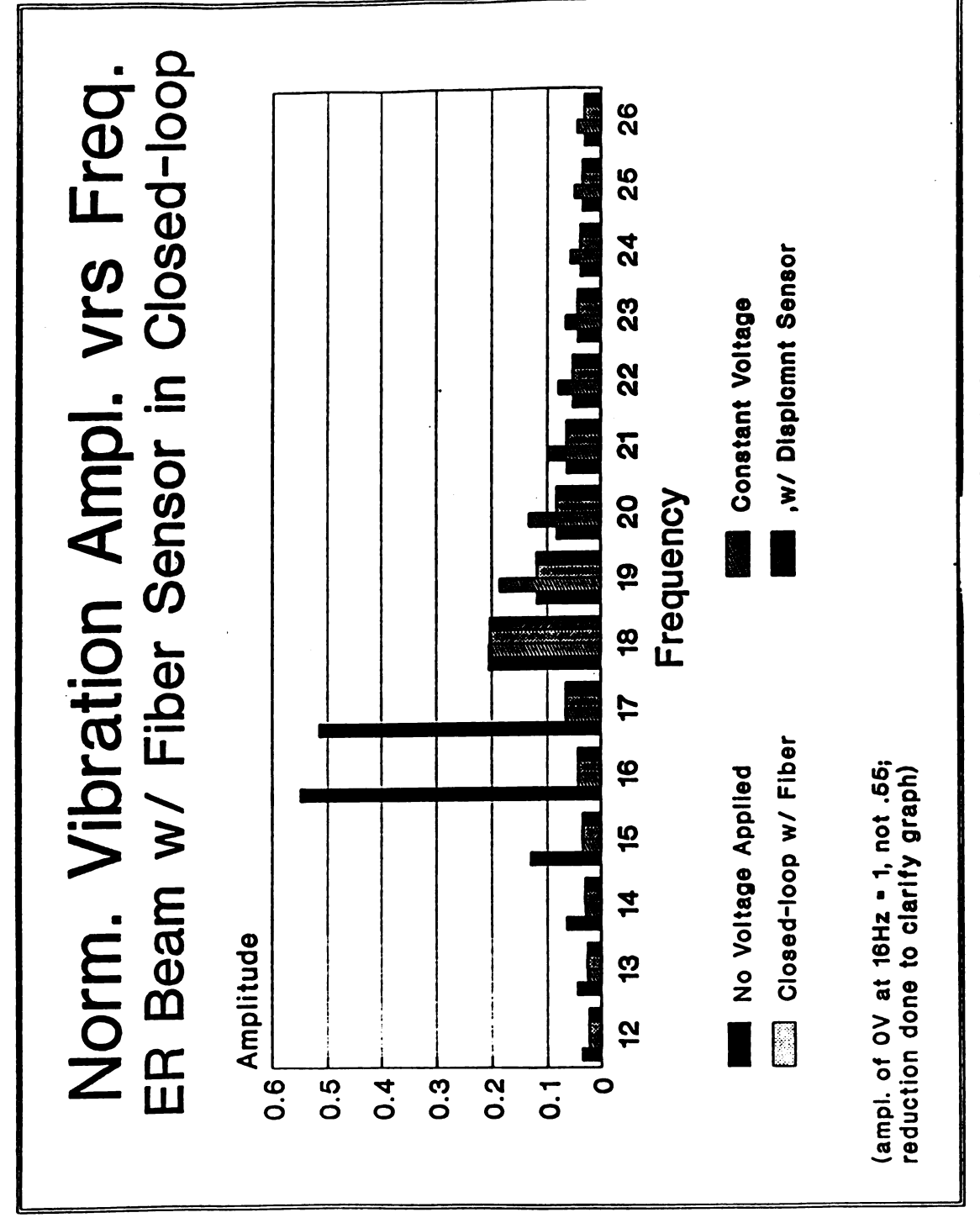


Figure 32: Normalized Vibration Amplitude vrs Exchation Frequency for Comparison of Natural Response vrs Smart Structure Response

#### CONCLUSIONS

Based on the results presented in this thesis, a number of conclusions may be drawn. Based on a review of the field, there is considerable research involving a wide variety of fiber-optic sensors and their incorporation into polymeric composite materials, but the description of methods undertaken to protect fibers during the cure process has been scant. The methods described herein represent a collection of and an improvement on the processes described previously.

Another innovation was the design of a fixture with several slits to allow several alike fringes to fall simultaneously upon a photodiode, which improved the signal strength in Mach-Zehnder and Michelson interferometric fiber-optic sensors.

Also, it was found that although standard, acrylate coated optical fibers are less durable at withstanding the cure temperatures than polyimide coated fibers, imbedded fiber-optic sensors composed of acrylate coated fibers did still function after undergoing the cure process. Thus, although sensors using specially coated fibers may have improved sensitivity and reduced impact on the composite structure when imbedded, fiber-optic sensors with standard coatings are suitable for imbedding in composite structures, as well as being less expensive and more available at the present time.

Another finding of interest was the dependance of the phase of the polarimetric sensor signal on the frequency of excitation of the beam the

sensor monitored. The phase offset differed for sensors of different lengths, and as a result, the use of the polarimetric signal was difficult for phase-based control methods. Also of interest was the reduction of the ER fluid effect with increasing shear strain as vibration amplitudes increased.

In addition to fiber-optic sensor research, there are many publications on the topic of vibration control with either ceramic or polymeric piezo-electric actuators, as well as some research on other actuators, such as electro-rheological fluids, shape memory alloys, and magnetostrictive materials. There have not, however, been many publications that bring such actuators together with fiber-optic sensors imbedded in polymeric composites and vibration control algorithms. This accomplishment is the subject of this thesis, and it is hoped that this will encourage further steps in the integration of diverse fields for the development of smart structures.

Forced vibrations in a cantilever beam with ER fluid were reduced over various forcing frequencies by as much as 95% using a surface-bonded polarimetric fiber-optic signal to a controller utilizing a look-up table control program. Similarly, forced vibrations at resonance in a carbon-epoxy beam with an imbedded single-ended polarimetric sensor and surface-bonded polymeric piezo-electric actuator were reduced by a factor of five.

## RECOMMENDATIONS

There is much work yet to be done to bring the systems described herein from the laboratory to practical applications in industry. One step in this process is the extension of the technology to two dimensions, where sensors and actuators are applied to to plates, for example. This involves more complex control schemes, and actuator placement is more complicated as well. This step is already in its initial stages of development by the authors.

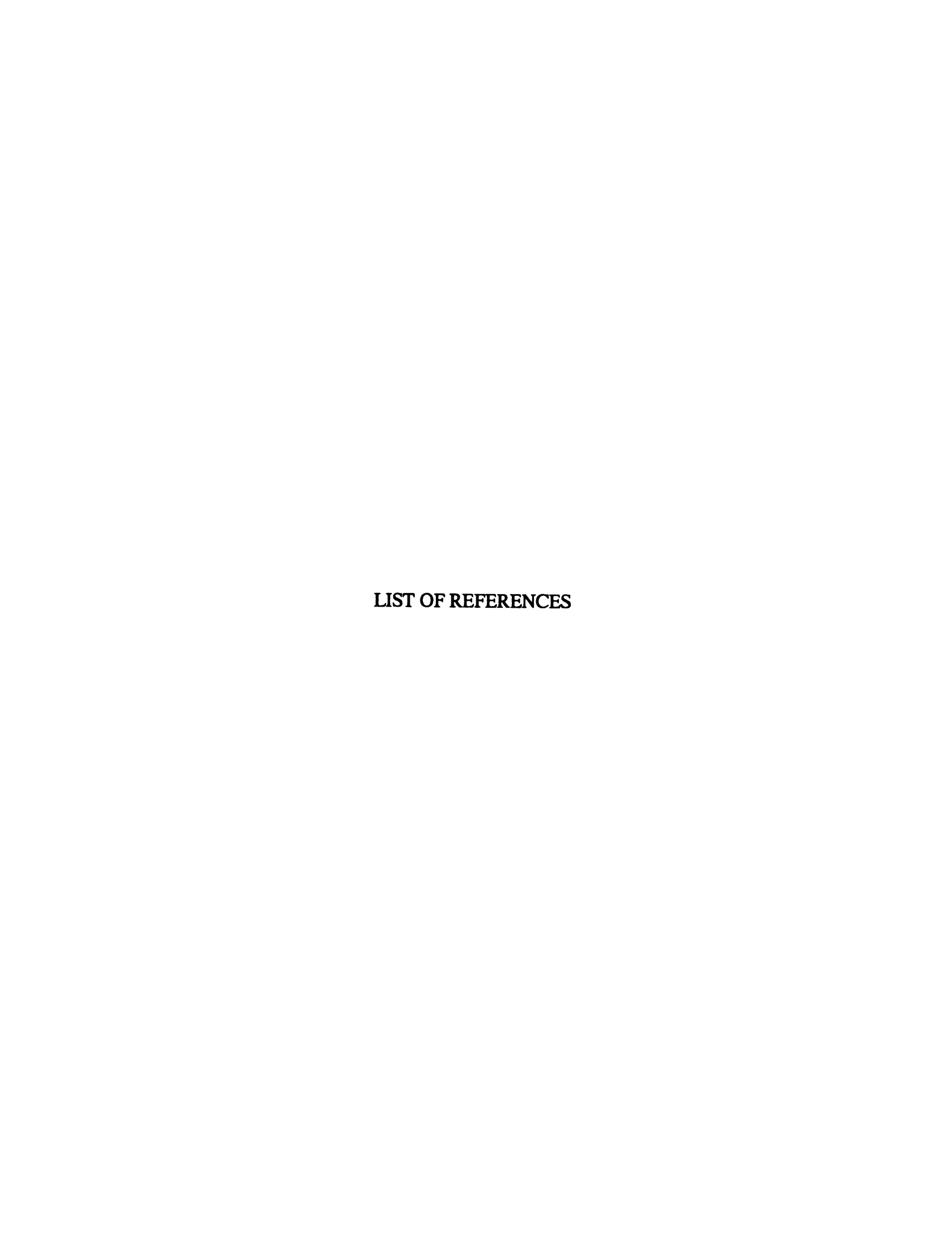
Another step in this process is the packaging of the 'smart structure' as a unit to allow installation by non-specialized personnel. This includes the assembly of preformed panels or other structures, with the sensors and sensors and actuators already incorporated. For example, the fiber sensors can be imbedded with pigtailed ends, for a simple mechanical connection to signal processing equipment.

Furthermore, the simple control algorithms used thus far could easily be replaced by more efficient programs, and eventually even adaptive neural networks could be used. Also, it would be best if the control software and hardware could be incorporated onto a dedicated integrated microchip, once specific control methods have been selected.

In addition, health monitoring of the structures may be accomplished with networks of strength-tailored fibers in the same structure where vibration control is accomplished. The initial research in this direction has already been accomplished<sup>1</sup>, but the health monitoring still needs to be tied in with other smart materials aspects.

Also, research into cure monitoring needs to be further developed than its current level in order to produce consistent, fully polymerized materials. This cure monitoring of polymeric composites may be accomplished, at least in part, with the same imbedded sensors which are to sense vibrational strains during the structure's post-cure service, although both pressure and temperature require monitoring. This advance has been at least partially accomplished according to the most recent issue of the NASA Tech Briefs<sup>33</sup>.

With these advancements and the research already accomplished the age of smart materials is just ahead, where the structures we build begin to look after themselves.



#### LIST OF REFERENCES

- 1. Measures, R.M. "Fibre Optic Sensors The Key to Smart Structures," Proceedings: Fibre Optics Conference 1989, pp. 1-14, SPIE Vol. 1120 (1989).
- 2. Turner, R.D., T. Valis, W.D. Hogg, and R.M. Measures. "Fiber-Optic Strain Sensors for Smart Structures," Journal of Intelligent Materials, Systems, and Structures, Vol. 1, pp. 26-49, January (1990).
- 3. Claus, R., C. DiFrancia, J.W. Hellgeth, and T.C. Ward. "Structure / Property Correlations of Several Polyimide Optical Fiber Coatings for Embedding in an Epoxy Matrix," Fiber Optic Smart Structures and Skins II, pp. 505-12, SPIE Vol. 1170 (1989).
- 4. Hogg, W.D., R.D. Turner, and R.M. Measures. "Polarimetric Fibre Optic Structural Strain Sensor Characterisation (sic)," Institute for Aerospace Studies, University of Toronto.
- 5. Valis, T., E. Tapanes, and R.M. Measures. "Localized Fiber Optic Strain Sensors Embedded in Composite Materials," Institute for Aerospace Studies, University of Toronto.
- 6. Field, S.Y., and K.H.G. Ashbee. "Weathering of Fiber Reinforced Plastics: Progress of Debonding Detected in Model Systems by Using Fibers as Light Pipes," *Polymer. Engrg. and Science*, 12:30-33 (1972).
- 7. Waite, S.R., R.P. Tatam, and A. Jackson. "Use of Optical Fibre for Damage and Strain Detection in Composite Materials," <u>Composites</u>, Vol. 19, No. 6, pp. 435-42, November (1988).
- 8. Rogowski, R., M. Holben Jr., J. Heyman, and P. Sullivan. "A Method for Monitoring Strain in Large Structures: Optical and Radio Frequency Devices," Rev. Prog. Quant. Non Destructive Evaluation, Vol 7A, pp. 559-63 (1988).
- 9. Martinelli, M., "The Dynamic Behavior of a Single-Mode Optical Fiber Strain Guage," *IEEE Journal of Quantum Electronics*, Vol. QE-18, No. 4, pp. 666-70, April (1982).
- 10. Waite, S.R. "Use of Embedded Optical Fibre for Early Fatigue Damage Detection in Composite Materials," <u>Composites</u>, Vol. 21, No. 2, pp. 148-54 (1990).

- 11. Hocker, G.B. "Fiber-Optic Sensing of Pressure and Temperature," Applied Optics, Vol. 18, No. 9, pp. 1445-8 (1979).
- 12. Lagakos, N., and J.A. Bucaro. "Pressure Desensitization of Optical Fibers," Applied Optics, Vol. 20, No. 15, pp. 2716-20 (1981).
- 13. Griffiths, R.W., and G.W. Nelson. "Recent and Current Developments in Distributed Fiber Optic Sensing for Structural Monitoring," SPIE O-E, *Fiber/Lase '88*, Boston; Paper No. 985-12 (1988).
- 14. Meltz, G., W.W. Morey, and W.H. Glenn. "Formation of Bragg Gratings in Optical Fibers by a Transverse Holographic Method," Optics Letters, 14:823-825 (1989).
- 15. W.B. Spillman, Jr., and B.R. Kline. "Fiber-Optic Vibration Sensors for Structural Control Applications," Hercules Aircraft Company, Damping '89 Conference.
- 16. Urruti, E.H., and J.F. Wahl. "Coatings Affect Fiber Performance in Smart Skin Sensing," Laser Focus World, pp. 165-70, January (1990).
- 17. Liu, K., M. Digonnet, K. Fesler, B.Y. Kim, and H.J. Shaw. "Superflourescent Single Mode Nd:Fiber Source at 1060 nm," Edward L. Ginzton Laboratory, FDD5-1, pp.462-5 (1987).
- 18. Crawley, E.F., and J. de Luis. "Use of Piezoelectric Actuators as Elements of Intelligent Structures," AIAA Journal, Vol. 25, No. 10, pp. 1373-85 (1987).
- 19. Crawley, E.F., and E.H. Anderson. "Detailed Models of Piezoceramic Actuation of Beams," Journal of Intelligent Materials, Systems, and Structures, Vol. 1, pp. 4-25 (1990).
- 20. Crawley, et al. "Development of Piezoceramic Technology for Applications in Control of Intelligent Structures," presented at American Control Conference, Alanta (1988).
- 21. Kynar Technical Manual, Pennwalt Corporation.
- 22. J.E. Hubbard, Jr., and T. Bailey. "Distributed Piezoelectric-Polymer Active Vibration Control of a Cantilever Beam," Journal of Guidance, Control, and Dynamics, Vol. 8, pp. 605-11 (1985).
- 23. Ikegami, R., D.G. Wilson, J.R. Anderson, and G.J. Julien. "Active Vibration Control Using NiTiNOL and Piezoelectric Ceramics," *Journal of Intelligent Materials, Systems, and Structures*, Vol. 1, pp. 189-206 (1990).

- 24. Baz, A., and S. Poh. "Performance of an Active Control System with Piezo-electric Actuators," Journal of Sound and Vibration, 126(2), pp. 327-43 (1988).
- 25. Gandhi, M.V., B.S. Thompson, and S.B. Choi. "A New Generation of Innovative Ultra-Advanced Intelligent Composite Materials Featuring Electro-Rheological Fluids: An Experimental Investigation," *Journal of Composite Materials*, Vol. 23, pp. 1232-55 (1989).
- 26. Gandhi, M.V., and B.S. Thompson. "A New Generation of Ultra-Advanced Intelligent Composite Materials Featuring Electro-Rheological Fluids,"

  Intelligent Materials and Structures Laboratory, Michigan State University.
- Sun, C.T., B.V. Sankar, and V.S. Rao. "Damping and Vibration Control of Unidirectional Composite Laminates Using Add-On Viscoelastic Materials," Journal of Sound and Vibration, 139(2), pp. 277-87 (1990).
- 28. Rogers, C.A., C.R. Fuller, and C. Liang. "Active Control of Sound Radiation from Panels Using Embedded Shape Memory Alloy Fibers," *Journal of Sound and Vibration*, 136(1), pp. 164-70 (1990).
- 29. Rashleigh, S.C. "Origins and Control of Polarization Effects in Single-Mode Fibers," *Journal of Lightwave Technology*, Vol. LT-1, No. 2, pp. 312-31, June (1983).
- 30. Burke, S.E., and Hubbard, J.E. Jr. "Distributed Parameter Control Design for Vibrating Beams Using Generalized Functions," Charles Stark Draper Laboratory, Cambridge, MA.
- 31. Memory Metals informational booklet, Memory Metals Inc., 1985.
- Rogers, C.A. "Novel Design Concepts Utilizing Shape Memory Alloy Reinforced Composites," Proceedings of the American Society for Composites, Third Technical Conference, Seattle, WA, pp. 719-31 (1988).
- 33. NASA Tech Briefs, p. 66 January (1990).

## General References

- 1. Allard, F.C., ed. <u>Fiber Optics Handbook For Engineers and Scientists</u>, New York, McGraw-Hill Publishing Co. (1990).
- 2. Daly, J.C., ed. Fiber Optics, Florida, CRC Press, Inc. (1984).
- 3. Hecht, E. Optics, Massachusetts, Addison-Wesley Publishing Co. (1987).
- 4. Waite, S.R., and G.N. Sage. "The Failure of Optical Fibres Embedded in Composite Materials," Composites, pp.288-94, July (1988).
- Wiencko, J.A., R.O. Claus, and R.E. Rogers. "Embedded Optical Fiber Sensors for Intelligent Aerospace Structures," Sensors Expo Proceedings, pp. 257-62 (1987).
- 6. Paipetis, S.A., and P. Grootenhuis. "The Dynamic Properties of Fibre Reinforced Viscoelastic Composites," Fiber Science and Technology, Vol 12, pp. 353-76 (1979).
- 7. Application Manual for the Design of Etrema Terfenol-D<sub>tm</sub> Magnetostrictive Transducers, Edge Technologies, Inc., prepared by J.L. Butler (1988).
- 8. Kashyap, R., and B.K. Nayar. "An All Single-Mode Fiber Michelson Interferometer Sensor," *Journal of Lightwave Technology*, Vol. LT-1, No. 4, December (1983).
- 9. Thompson, B.S., C.Y. Lee, and M.V. Gandhi, Intelligent Materials and Structures Laboratory research results.
- 10. Claus, R.O., B.S. Jackson, and K.D. Bennett. "Non Destructive Testing of Composite Materials by OTDR in Imbedded Optical Fibres," *Proceedings, SPIE Int. Symposium*, San Diego, August (1985).
- 11. Rogers, A.J. "Distributed Optical-Fibre Sensors," Journal of Physics D: Applied Physics, Vol. 19, pp. 2237-55 (1986).

AICHIGAN STATE UNIV. LIBRARIES